IDENTIFICATION AND CHARACTERIZATION OF ACTIVE FAULT BY SPACE BORNESCAN SAR INTERFEROMETRY AND GROUND BASED GPR TECHNIQUES IN NW HIMALAYAN FOOT HILL REGION, INDIA

Thesis submitted to

Andhra University
(Visakhapatnam)

in partial fulfillment of the requirement for the award of

Master of Technology
in
Remote Sensing and GIS

Submitted By:
Rohit Kumar

Supervised By:
Dr. R.S Chatterjee, Scientist 'SG', GSDMS

Indian Institute of Remote Sensing,
Indian Space Research Organization,
Dept. Of Space, Govt. Of India,
Dehradun - 248001, Uttarakhand, India

- AUG, 2015-

Dedicated to my beloved Parents

DISCLAIMER

This document describes work undertaken as part of a programme of study at the Indian Institute of Remote Sensing of Indian Space Research Organization, Department of Space, Government of India. All views and opinions expressed therein remain the sole responsibility of the author, and do not necessarily represent those of the Institute.

ABSTRACT

The study of active fault is the process to understand the current tectonic movement in high seismic zone areas like Himalayan Frontal Thrust. Identification and characterization of the tectonically active area by geomorphological criterion was applied in the study area. An attempt has been made out to find the relationship between geomorphological indicator and active fault location which was verified by geophysical techniques, Ground Penetrating Radar. Topographic analysis using Digital Elevation Model was done to detect subtle change in elevation in piedmont area, Drainage anomalies were identified and analyzed to identify the location of faults and lineaments, some of which may be active as manifested by multi-temporal data analysis. This also facilitates the site selection for GPR survey. Geomorphic signatures of active tectonics such as fault scarps, topographic breaks, knee bends in rivers, and sudden termination of alluvial fans, sag ponds and steep river terraces were observed in the field. GPR technique was used to confirm surface subsurface faults based on the offset of depositional layers and thereby to relate with the surface indicators. The survey was carried out in transverse direction to the suspected faults. Some of the sites clearly show fault characteristics as indicated in radargram as change in frequency/amplitude of the radar signal and abrupt change in radar facies.

SAR interferometry method was attempted to decipher strain accumulation zone with ScanSAR differential Interferometry procedure. The advantage of ScanSAR is the ability to achieve wide-swath coverage (about 350km swath) with moderate resolution 100 m to address wide-ranging crustal movement caused by active motion of the Indian plate. With present study ScanSAR data pair was successfully processed and attempt were made to use primary observation on deformation related to active tectonic of Himalaya.

Keywords: Himalayan Frontal Thrust, Drainage anomaly, Topographic Anomaly, Active fault, GPR, ScanSAR Interferometry, Crustal Deformation, Earthquake.

ACKNOWLEDGEMENTS

I would like to thank Dr. A. Senthil Kumar (Director, IIRS), Dr. Y.V.N Krishnamurthy (former Director IIRS) Dr. SPS Khushwaha (Dean Academics, IIRS) Dr. S. K. Saha (Former Dean Academics, IIRS) and all IIRS faculties, staff for providing a nice infrastructure and environment to carry out the present research work.

I want to extend my deepest gratitude to my thesis supervisors Dr. R.S Chatterjee, Senior Scientist, Geosciences and Geohazards Department from IIRS for their constant support and priceless guidance throughout my research and course work.

I thank Dr. P. K. Champati Ray (Head, GSGHD) for his valuable suggestions for this project work.

I would also like to thank all the scientists in GSGHD and the M.Tech course Director Ms. Shefali Agarwal for their support during this course.

I would like to express my heartfelt gratitude to all faculty of Geosciences and Geohazards Department, specially Dr. Shovan Lal Chattoraj, Ms. Richa Sharma, Mr. Suresh Kannaujiya and former faculty Dr. Ajanta Goswami for his valuable advice, continuous encouragement and moral support during the entire course.

I humbly acknowledge the help from Dr. Ashutosh Bhardwaj (Scientist, PRSD) for sharing DGPS data during the initial days of this research.

I specially thank Miss Somalin Nath (Researcher, GSGHD), for providing me important literature, materials, giving me support for the things which I wanted to do in my research work and for always motivating me.

My special thanks to the non-teaching staffs Mr. Ashish Dhiman, Ms Sushama, Ms Ramandeep for their extreme support given to me during this project. I am also thankful to my classmates and reserchers Pratiman, Gaurav, Anant, Ankur, Mayank, Aniket, Unmesh, Vikrant, Sumi, Shobhana, Chayanika Bhavana, Vivek, Gopal, Shaileja and Surojit Dada for all the good times spent during my stay at IIRS.

I sincerely thank the entire team of Computer Maintenance Department for taking care of all the system and software needs. I thank Mess workers for the great hospitality and food arrangement, Security personals for their coordination in the last two years at IIRS.

Lastly, I offer my regards to all of those who have supported me in any respect during the completion of this research work.

Rohit Kumar

CERTIFICATE

This is to certify that **Rohit Kumar** has carried out the dissertation entitled **"Identification and characterization of active fault by space borne ScanSAR interferometry and ground based GPR techniques in NW Himalayan foot hill region, India"** for the partial fulfillment of the requirement of **Master of Technology in Remote Sensing and Geographic Information System** from Andhra University.

This work has been carried out at **Geosciences and Geo-hazards Department, Indian Institute of Remote Sensing, (ISRO)**, Dehradun, India under the supervision and guidance of **Dr. R.S Chatterjee** of IIRS, Dehradun. This report contains the original work carried out by him in the academic session **2013-15** and he has duly acknowledged the sources of data and resources used.

Dr. P. K. Champati Ray
Group Head GSDMS & Head GSGHD
IIRS, Dehradun

Dr. R.S Chatterjee
Senior Scientist
Geosciences and Disaster management studies,
IIRS, Dehradun

Dr. S. P.S. Khushwaha
Dean (Academics)
IIRS, Dehradun

Dr. A Senthil Kumar
Director
IIRS, Dehradun

TABLE OF CONTENTS

LIST OF FIGURES

LIST OF TABLES

List of Abbreviations

ALOS	Advanced Land Observation Satellite
ASTM	American society for Testing and Materials
DEM	Digital Elevation Model
DGPS	Differential Global Positioning System
DInSAR	Differential Interferometry Synthetic Aperture Radar
GIS	Geographical Information System
GPS	Global Positioning system
HFT	Himalayan Frontal thrust
IDS	INGENERIA DEI SISTEMI S.p. A)
InSAR	Interferometric Synthetic Aperture Radar
ITSZ	Indus Tsangpo Suture Zone
LISS	Linear Imaging Self Scanning Sensor
LOS	Line of Sight
MBT	Main Boundary Thrust
MCT	Main Central Thrust
RS	Remote sensing
SAR	Synthetic Aperture Radar
SRTM	Shuttle Radar Topography Mission
WB	Wide Beam

1 INTRODUCTION

1.1 Background

The Himalayan Frontal Thrust (HFT) is tectonically most dynamic regions located at the southernmost edge of the Sub-Himalayas. It is measured as a one of the most significant key area where the transfer bends caused by collision of India with Eurasia. Different techniques like GPS evaluation and Plate movement representation etc., reveals that India Eurasia convergence go on with in the present day at a rate of approx about 40 to 50 mm/year. However the remaining movement is absorbed by a combined effect of folding faulting of thrusting, within the Eurasian plate. (DeMets, et al., 2010) (Paul, et al., 2000). Four enormous Himalayan earthquakes like Assam-1897, Kangra-1905, Bihar-1934 and Assam-1950 in the frontal belt are the most powerful manifestation of the state of high tectonic flux in the region. Active faults are common features in the frontal zone, they appear mainly along the HFT. Thus, HFT shows wide active faulting area and associated uplift which represents a zone of active deformation between the Siwalik Hills and the Gangetic Plain. Himalayan river system transported much more sediments and deposited at the foot of the range, and developed alluvial fans and river terrace during the last diastrophism of outer Himalaya and thereafter. Formation and deformation of such geomorphic surfaces along the Himalayan foothills suggest that the last orogenic movement of the area is still ongoing and highly active. (Yeats, et al., 1992) (Nakata, 1972)

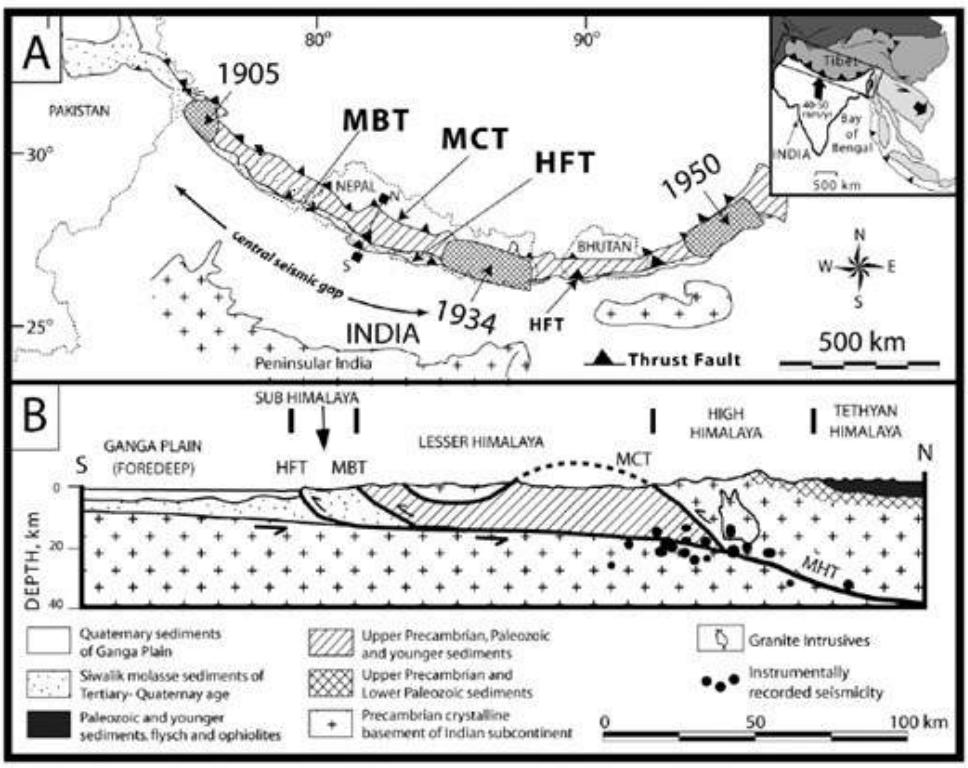

Figure 1 Himalayan thrust location with great earthquake location and Generalized North south Geological section (Kumar , et al., 2006)

Fig. 1 A. Tectonically active zones (MBT, MCT, HFT) and major earthquakes (1905 Kangra, 1934 Bihar-Nepal and 1950 Assam)
Fig. 1B. Geologic cross section of the central Himalaya region, Sources (Kumar , et al., 2006)

The study of active fault is the process to understand the current tectonic movement in high seismic zone areas like Himalayan Frontal Thrust. In this study, we investigated Geomorphological, especially drainage analysis and topographical profiling using remote sensing temporal data and Digital Elevation model (DEM) studies over five basin in Himalayan piedmont plain and correlation between them with Ground penetrating radar has been attempted. GPR is high resolution nondestructive technique which based on electromagnetic waves was very useful and rapidly mark the subsurface structure. The drainage analysis, topography analysis, lineament mapping and geological mapping and its combined effect are conclusive technique for identifying probable subsurface active fault. Collective information of active fault is successfully traced in radar profile (GPR) techniques. SAR interferometry methods is verified techniques to surface deformation measurement. In this study attempted to establish the crustal strain accumulation zone with ScanSAR differential Interferometry procedures. The benefits with ScanSAR is the capability to achieve wide-swath coverage, moderate resolution and extensive range crustal motion extraction and strain accumulation region (Liang, et al., 2010) which caused by active motion of Indian plate.

1.2 Need of the study

The Himalayan foothills are one of the most densely growing populated area of India. It lies under seismic zone IV. In spite to its high vulnerability, HFT was traditionally considered of low seismic hazard. Current historical catalogue lists very few large earthquakes in the area and show that most of them do not exceed Mw 6. Most of the seismicity is concentrated between HFT and MBT area. Since even moderate earthquakes can produce extensive damage due to the high exposure of the building and facilities, the identification and characterization of potential seismogenic sources are crucial for mitigation of seismic risk. The study of faulting is not just an academic profession. The fault must be studied carefully because faults and fractures play an important role in tectonic boundary area. Regional fault analysis is required for the localization and building of large human-made structures, such as dam and nuclear power plants. Such structures, which may have devastating impact when they fail, should clearly not be built near potentially active fault. But perhaps the most dramatic effect of fault activity on society comes in the form of earthquakes, which can be responsible for great loss of life and can destroy the economic stability of developing countries. Studying active faults is useful for

- Estimating Natural Hazard (Seismic, Mass wasting) and other geological hazards (disastrous sedimentation and erosion);
- Research of recent Geodynamics;
- Interpretation of more prehistoric tectonics by comparison with the recent ones.

1.3 Problem statement and Motivation

The aim of this work is to efficiently identify tectonically active zone with high strain accumulation which leads to active faulting in the zone and relevant to the Earth surface motion by combining information from geomorphological analysis, Ground Based GPR (Ground Penetrating Radar) profiling and SAR Interferometry.

Himalayan region is one of the most seismically active areas of the earth because of the constant northward movement of the Indian Plate towards Eurasian plate at the rate of 40 mm per year that has produced the three major fault systems (MCT, MBT, and HFT). Devastating earthquakes have been observed in this region (6.8 Mw Uttarkashi 1991, Chamoli 1999, and Kashmir 2005). The areas around the Himalayas are classified under zones IV and V which are the highest seismic risk regions of India, it is the major hazardous region in the world due to high crustal deformation, high upliftment and high incision and erosion rates. On another hand Himalayan region has unprecedented potential difference in terms of population and development, particularly hydropower projects, nuclear power project infrastructure and urban centers, thereby making it one of the high risk zones in the world. The HFT marks the principle tectonic displacement zone at the northern boundary of the stable Indian Plate.

Active faults and seismic hazard evaluation in the tectonically active outer Himalaya are crucial because of the increasing urbanization and population growth in the foothills and in the adjacent plains. The source of the active faults is the strain accumulated along the fault plane caused by the plate motion. But some of active faults near the plate boundary may react and generate large earthquakes soon after the larger earthquakes on the plate boundary. We need to know the amount of stored energy and the size of the fault, which would eventually fail to release the energy.

ScanSAR has an excellent outlook in the extensive range of examination. In adding up to ScanSAR data it can also be used for interferometry which makes the wide range surface deformation observing easier to execute. . The use of GPR became an instrument favoured by geologists for its non-destructive capabilities and its ability to survey large areas more quickly than conventional methods (drilling, Trenching. etc.)

1.4 Aim and objectives

In this work, the research strategy focused on the geomorphological study using remote sensing and geophysical (GPR) techniques including field studies to examine and understand active faults and how they relate to spatial patterns and progress of natural hazards, particularly earthquakes, in NW Himalayan foot hill region.

A number of objectives have to be accomplished in order to fulfil the aim

1.4.1 Research Objectives

- To identify relative zonation of tectonic activity and probable locations of active faults using geomorphological analysis.
- To study deformation associated with the horizontal plate movement related strain accumulation in and around the major thrust zones (HFT, MBT) using spaceborne SAR interferometry techniques
- To identify and characterize active faults by ground-based GPR survey.

1.4.2 Research Questions

- How Drainage, Topographic anomalies are helpful for identification of tectonic activities in Piedmont areas.
- How far GPR can be used to investigate active subsurface piedmont faults?
- How ScanSAR interferometry are useful to decipher horizontal deformation of active tectonics of the Himalaya?

1.5 Thesis Outline

This thesis offers a methodology that combines geomorphological indicator with Space borne Interferometry and Ground penetrating radar data, to assess the tectonic setting and activity level of areas with active crustal deformation.

Chapter 1. Briefly describe importance of the study, motivation, research objectives and question.

Chapter 2. Literature review and theoretical background about the earlier work.

Chapter 3. Defines the necessity of the study area, different datasets and field survey instrument used in the study.

Chapter 4. The chapter four describes the adopted methodology working in this present work in detail.

Chapter 5. The fifth chapter explains and discusses all the Results obtained in this present study.

Chapter 6. The chapter six is the Conclusions and future Recommendations.

2 LITERATURE REVIEW

The literature relevant to this thesis is considered in five separate sections viz., the first three relating to geology geomorphology and active tectonics of the study are (Section 2.1, 2.2 and 2.3) and the fourth which relates to the geophysical techniques GPR used in the study especially when applied to subsurface structure analysis (section 2.4) and the last (section 2.5 is) related to SAR interferometry techniques focus on ScanSAR interferometry.

2.1 Himalaya

2.1.1 Geodynamic Setting of the Himalaya

The northwest ward movement of The Indian plate and collision between Eurasia plates constructed the Himalayan mountain arc system which stretch 2,500 km (1,500 mi), from Kashmir in the West to Arunachal in the East. In the primary phase Tethys Sea situated at southern part of Eurasia plate, which separated of the two continents. The collision of Indian plate with Eurasian plate produced the world highest topographic landscape on globe

Sub-division of Himalaya

The Himalayan orogeny classified based on the criterion of geography, stratigraphy, structure, and political. Observation of Ganesser, Wadia, Lefort, the Himalayan region categorized into four geological Unit. These units are supposed to continuous along the whole Himalayan structures.

- The Sub-Himalaya Zone (Tertiary divisions);
- Lower Himalaya Zone (nonfossiliferous low-grade metamorphic rocks; it is also known as the Lesser Himalaya,;
- Higher Himalayan Zone (crystalline complex consisting of gneisses and aplitic granites; it is also known as the Greater Himalaya; and
- Tethyan Himalayan Zone (marine, fossiliferous strata).

The sub-Himalaya region composed of mainly Himalayan river deposit and diastrophism. The Siwalik Hills are the product of folding, faulting and upliftment of sub-Himalaya rocks. Along the MBT, Lesser Himalayas rocks have been under-thrust by sub-Himalaya. In the sub-Himalaya area the process of diastrophism begun during Pliocene time and has been presented as dynamic through the Pleistocene. The Himalayan frontal thrust (HFT) is south boundary of the Sub-Himalaya rocks.

Lesser Himalaya region is restricted by Main Boundary Thrust (MBT) and Main Central Thrust in south and North respectively. In lesser Himalaya major rock units is green-schist metamorphism rocks, and sedimentary rock varieties from Indian plates. Sequence of anticlines and synclines are presented in lesser Himalayan region.

The Central Crystalline Zone, contained of ductile distorted metamorphic rocks and marks the axis of orogenic uplift is recognized as Higher Himalayan zone. The main rock variety in

topmost higher Himalayan zone is Mica schist, quartzite, parageneiss, migmatites and leucogranite. These rocks represents a multiphase distortion results, the initial existence Barrovian type, or ordinary geothermal gradient situation. Main central thrust (MCT) is connected north to south direction along deformation zone, which conveys the Higher Himalaya on top of the Lower Himalayas.

The boundary between Eurasia and Indian plate or northern boundary of Himalaya marked as Indus-Tsangpo Suture Zone (ITZS). Main rock criterion of theses zone are ophiolites and ophiolitic complexes.

The Himalayan progression has been largely separated into two phases (a) The Eo-Himalayan event that happened during the middle Eocene to Oligocene (45-25 Ma) and the, (b) The Neo-Himalayan event that occurred the early Miocene. Stratigraphically, the Himalayan Orogeny consists of the Neogene Siwalik Group, the Lower Himalayan Sequence (LHS), and the Proterozoic-Ordovician Greater Himalayan Crystalline Complex (GHC) and the Proterozoic to Eocene Tethyan Himalayan Sequence (THS). The major Tectonic-stratigraphic units in the Himalayan orogeny are separate as the Main Frontal Thrust hanging wall, Main Boundary Thrust hanging wall, Main Central Thrust hanging wall, and South Tibetan detachment hanging wall.

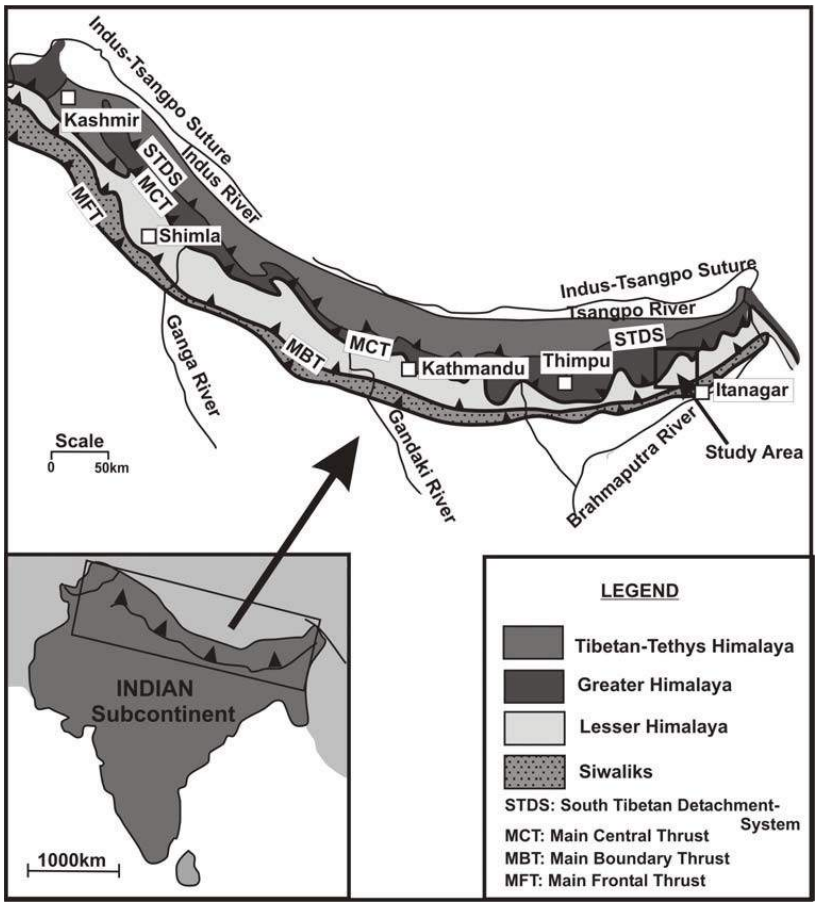

Figure 2 Major Division of Himalaya (Picture taken From IITK repository)

Major structure of the Himalaya

The Himalaya orogeny characterize one of the major tectonic zones in earth, where a continental crust under-thrust another continental crust. The total length of Himalayan arc is 2500 km long, between 75°E and 98°E, Covering from Kashmir to Arunachal Pradesh due to collision of Eurasia and Indian continents. Due to movement of Indian land mass toward northwest direction the underneath sedimentary masses with its solid basement was under multiple deformation and divided by faulting, folding and thrusting. (Kayal, 2014). The deformation contact zone from northern to southern is the Indus Suture Thrust (IST), the Main boundary Thrust (MBT), The Main Central Thrust (MCT) and the Himalayan Frontal Thrust (HFT). The IST represents the junction of two continents collision region. Main central thrust (MCT) is the fault system that develops along the south part of Higher Himalaya and separated the higher Himalaya between lesser Himalayas. Likewise Main Boundary thrust (MBT) is north dipping series of thrust fault situated on the south part of the lesser Himalaya and separated the sub-Himalayan rocks. The Himalayan frontal thrust identify the north dipping thrust fault system which separated the Himalayan orogeny to Indian plate.

2.1.2 Geomorphology of Himalaya

Geomorphology of Himalaya are controlled by surface upliftment, Plate tectonics setting, climate variation and exhumation processes. Himalayan region have great diversity in height variation in south to north followed by Himalayan foot hill region 640 m. to greater Himalaya 8,850 m. from MSL, the change in altitude and climate factor effected in regional Himalayan geomorphology. Plate tectonic setting; The continent collision between Eurasia and India produce world highest mountain, collision begun about 50 Myr ago but present movement of Indian plate beneath Eurasian plate cause upliftment of young mountain. Precipitation; the monsoon effect in Himalaya is the major factor of mass wasting. Slope instability, drainage density, fluvial action, effect the regional landscape in Himalayan region. In sub Himalayan region where mountain building movement are high reflected in fluvial geomorphological surface where River Terraces, old alluvial remanent reproduces the break of the continuous production of fluvial surface. The sequence of depositional and erosional process of fluvial agent controlled by tectonics uplift movement and monsoonal variation in Himalayan foot hill region. (Nakata, 1972). The rivers of foot hill zone are clearly indicate the active tectonics zone by drainage deflection, along the fault/thrust line, uplifted block of old alluvial remanent.

2.1.3 Overview of Himalayan Frontal Thrust

The progression of Himalayan foot hill landforms is orderly by slow tectonic change and river geomorphology, multi cyclic geomorphic surface gives the surface indicator of break in old alluvial plain. The Himalayan Frontal Thrust divides the Sub-Himalayas from the Lower Himalayas. Width of lower Himalaya is 60 to 70 km and altitude of lower Himalaya is 2,000 to 3,300 m (Nakata, 1972). These ranges contain of unfossiliferous Palaeozoic and Mesozoic formations of extremely tectonic deformed formation. South margin of lesser Himalayas are

thrust over the sub-Himalaya along the HFT. Sub-Himalayas average altitude is 1,300 m in elevation and width is 10 to 90 km, dominated by Siwalik formation (the Molasses of the Himalayas. The distortedly folded bedding plane primarily dipping in direction of north indicate the Siwaliks zone, dissimilar structure pattern and alignment of deposited feature make difference with sub-Himalayas. The HFT and surrounding area are primary place of deposition because of abrupt change in high relief to low relief area and geomorphic factors. The strong lineament indication presented in southern part of Himalaya shows that same origin as other margins boundary. The HFT region categorized on the basis of their geologic structure and geomorphological characteristics which indicate different type of lithological formation and crustal movements on different foothill region. HFT region is described by mainly three types of structures area, the piedmont are located in northern part of Indo-Gangetic Plain made by Khadar and Bāngar soils. Dun is special type of longitudinal depression between Siwalik and lesser Himalayan region, somewhere dun area are not present along Siwalik because lesser Himalaya and Siwalik are merged with each other. And last one is Re-entrant types, which means a surface is made with two parallel ridges in low elevated area. Piedmont zone are dominantly presented in Eastern Himalayas, Dun are presented where Siwalik and lesser Himalaya separated by valley in Central Himalayas, the last one western Himalayas is cover by Re-entrant Type. (Nakata, 1972).

2.2 Active Fault Study

Active fault study is a critical initial step in the analysis of the high seismic zonation of area like active Himalayan frontal thrust where Urbanization and population growth are higher because of highly fertile Indo-Gangetic plane. Active fault study is not only belongs to educational/research area, Industrialization. In the study of active fault we take to consider a factor of social objective (People, Society), geologically (Earthquake, landform) and Time.

2.2.1 Definition of Active fault

Different definition were given by several Researcher in the Area of active fault.

(Sherard, et al., 1974) (Allen & Cluff, 1975) has worked on motion of fault in the area of Dam basement, they suggest dam site should not be on active fault or not near the potentially active fault it may be cause of major earthquake trembling. According to Allen study an active fault (or a potential active fault) which have movement within the past and upcoming displacement with a 100 years.

(Wallace, 1990) USGS, has defined the displacement in past or coming future connected to society cause by fault is identified as Active fault. The age of fault associated to fault break, fault displacement, fault movement, fault slippage, and faulting result of shearing movement of ground on one side of fault against the other. Commonly the faulting/fracturing occur during a strong earthquake and, in fact, it is the energy release associated with the faulting which causes the earthquake.

(Trifonov & Machette, 1993) observed in the major project "World Map of Major Active Faults" that active fault which movement record on Holocene Epoch (12,000 to 11,500 years),

and late Pleistocene, present-time or another indicator of motion. Global Seismic Hazard Assessment Program (GSHAP) is useful for mapping of fault activity, identification of seismic zone.

(Yoshioka, 2009) suggested the study of active fault is beneficial for earthquake affected country like japan, and importance of active fault analysis for earthquake damage prevention. He said that future earthquake may be predicted by study of past fault movement.

A New Zealand's Earthquake Group worked on active fault and recommend the active fault is potential source of destructive earthquake hazard and decrease the damage of earthquake hazard not built the any large infrastructure within a radius of 50 km.

(Verma & Bansal, 2013) have addressed the importance of active fault investigation and seismic hazard estimation in developing nation like India where higher population growth and rapid infrastructure. Indian subcontinents has different tectonic setup from south to north, the historical time earthquake hazard also point out the loss of human life & property. He pointed the 1819 kachchh (Allah Band), the great Shillong, Bhuj (2001), Bihar (1934), Assam (1950), Kashmir (2005), and many more earthquake and their relation between active faulting. The active fault which active in current geological regime it may be reactivate in future time.He suggest the earthquake hazard estimation we need to identify and characterize the active fault with help of new technique GPS, InSAR and GPR.

(Philip, et al., 2014) defined the "active faults which have moved repetitively in current geological time have possible for reactivation in the future and they contribute significantly to 80% seismic activity."

2.2.2 Active Fault classification Criteria

The Fault activity, classification criterion can be determined by of fault movement in certain time interval, slip rate of faulted block, slip per event, and rupture length of fault plane and earthquake magnitude size. Key factor of fault movement determined by cumulative displacement over certain geological past time (see diagrams below) so may be estimate that the future fault displacement.

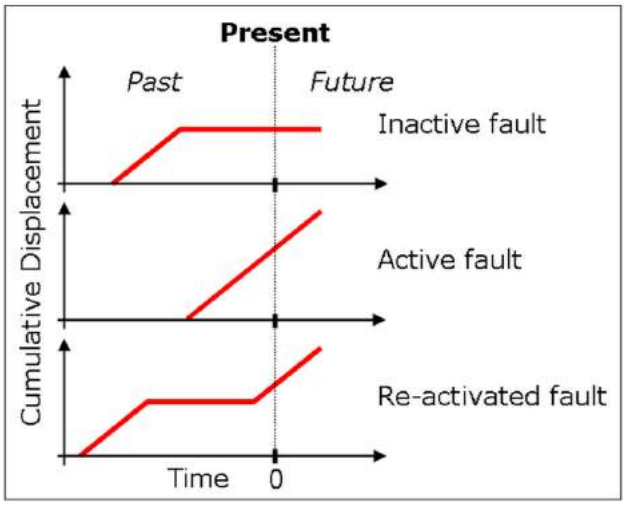

Figure 3 Fault activity relation with displacement

The significance characteristic of active fault are fault type and its geometry, basement rock and direction of tectonics movements, strain build-up, and complexity of major fault zone.

a. Slip Rate

A slip rate is calculated when a one side of the fault block travels with respect to the other side of fault block. The slip rate of rock mass is the average speed of total deformation always across fault plane. Slip rate across the fault is primary understanding of the global tectonics movements or local crustal deformation. Slip rate also reveal the fault location change in particular time. Slip rate calculate by given formula.

$$Average\ slip\ rate = \frac{Total\ distance\ coverd}{Total\ Time\ accuried}$$

b. Slip per Event

Slip per event describe the amount of change in particular fault break result, the amount of fault slip is varies to geological condition. The change in quantity of displacement are directed by amount of strain release and geometry and arrangement of faulting. Historical faulting event or prehistoric rupture event can be measure by geological and geophysical field investigation for measuring the amount of slip per event. In thrust faulting the vertical separation is measure as a vertical displacement.

c. Rupture length

The Rupture length is a product of faulting event and strongly correlated with earthquake size. An analysis of historic earthquake suggest that a large earthquake is produces large rupture length or a bigger fault rupture event gives the large magnitude earthquakes.

d. Earthquake Size

The earthquake size criteria reveal the fault activity, fault geometry and based on maximum intensity of quake and ground trembling. Seismicity of area connected to stationary constraint of an earthquake, shear modules including Rupture area and fault displacement. The comparison of fault activity based historic earthquake size.

e. Recurrence Interval

Fault recurrence Interval useful to characterize the earthquake occurrence as an average time between historical times. Historical recorded earthquake data gives a best clue about recurrence interval of movement. Fault activity and earthquake recurrence interval of earthquake is strongly correlated but it’s not depends on all fault system movement. Every Active fault movement has a different recurrence interval and it may be measured by using slip rate and displacement (offset of fault plane) in earthquake event.

Based on above criteria Wallace classified an active fault in 6 basic class and 5 sub-classes, the subclasses are similar to major classes, but major difference between fault behaviors. Table showing the active fault classification criteria.

Fault Classification Criteria

			Slip rate	Slip per event	Rupture Length	Seismic Moment	Magnitude	Recurrence Interval
Class-1	Class-1		>10 mm/yr.	>1 m	>100km	>10^{26} dyne-cm	>Mw 7.5	<500 yrs.
	Sub class 1	Class 1A	>5 mm/yr.	>1 m	>100km	>10^{26} dyne-cm	>Mw 7.5	<1000 yrs.
		Class 1B	10 mm/yr.	< 1m	>100km	>10^{26} dyne-cm	<Mw 7.0	<100 yrs.
Class-2	Class-2		1-10mm/ yr.	>1 m	20-200 km	>10^{25} dyne-cm	>Mw 7.0	100-1000 yrs.
	Sub class 2	Class 2A	1-10mm/ yr.	<1m	20-200 km	>10^{25} dyne-cm	<Mw 7.0	<100 yrs.
		Class 2B	1-10mm/ yr.	>5m	>100 km	>10^{25} dyne-cm	>Mw 7.0	>1000 yrs.
Class-3	Class-3		0.5- 5 mm/yr.	0.1-3 m	10-100 km	10^{24} dyne-cm	>Mw 6.5	500-5000 yrs.
Class-4	Class-4		0.1-1 mm/yr.	0.01-1m	1-50 km	10^{24} dyne-cm	>Mw 5.5	1000-10,000 yrs.
	Sub class 4	Class 4A	0.1-1 mm/yr.	>5 m	10 km	10^{25} dyne-cm	>Mw 6.5	1000-10,000 yrs.
Class-5	Class-5		< 1mm/yr.					> 10,000 yrs.
Class-6	Class-6		<0.1 mm/yr.					>100,000 yrs.

Figure 4 Fault classification criteria

2.2.3 Active Fault Study in India

Active fault study in Indian region is essential part of hazard evaluation and perdition because Indian continents has a great diversity from south to north and east to west. Several author have been worked on different part of Indian continents.

(Raj, et al., 2003) have worked on Lower Narmada valley to identify the active tectonism study of the tributary river basin (Karjan Basin). The main focus of the study using Morphometric Indices to measure Holocene movement in the area of Narmada rift fault zone. They calculated the MFS (Mountain Frontal Sinuosity), Vf ration (Valley floor rations), Valley floor width ratio, Lineament analysis, topographic profile variation and result was verified by field studies however the result of the integrated approach morphological analysis, geological and structural analysis gave clear evidence of active tectonics in lower Narmada valley .

(Morino, et al., 2008) have Observed and trenching along the Katrol Hill Fault ,Gujrat, the prime emphasis of this study was demarcate and delineate the probable new active fault along past rapture zone by using Satellite data interpretation and verified by GPR Techniques. The Kachchh area facing enormous earthquake in past time "(Allah Bund earthquake, Mw. 7.8; Anjar Earthquake Mw. 6.0 and Bhuj earthquake Mw. 7.6)" and probable to reactivate again in future time also in time of Bhuj earthquake its proved that Bhuj earthquake is not activated by active fault but also contribution of blind fault. They successfully mapped the reactivated old fault in the bank of Khari River near Wandhay Dam, the mapped fault characteristic showing three phase of deformation occurred in past Holocene time.

(Radhakrishnan , 2011) used data from DGPS campaign to Identified the Active fault plane in stable western Maharashtra region, the study carried out using DGPS survey in campaign mode to assess the stress-strain situation in the Koyna and Warna and its neighboring region, the research method of this study combing the result of GPS, seismic data and geological structure gives the activity of left lateral strike slip faulting along Koyna region. Therefore the results proved that the GPS data and other geological information sufficient to quantify the active tectonics zone in area of stable old region like peninsular area.

(Copley, et al., 2014) have observed the alluvial fan break as an indicator of active tectonics in the study area. The prime focus of the study was to describe the activity of the peninsular area which geologist know as a stable craton. Copley successfully mapped the "Tapti" active fault that may be dislocated by prehistoric earthquake.

2.2.4 Relationship of Active Fault and Earthquake

Among Social community it's a very common perception or myth that fault mean slip and slip leads to earthquake. This is one of the very familiar reason to become panic after hearing that fault is found near around the home. Extensively fault exists in the crust. After a research geologist came with that conclusion that inactive faults numbers are high in comparison to active ones. Inactive faults haven't slipped for a long time and the probability of there to become active in near future is also low. An on the other hand active fault as the name it defines which are recently active or slipped and the probability to slip again is high. Other common misperception is that all slip or activity triggers the earthquake. If it triggers the earthquake we call it seismic fault but if it doesn't trigger the quake than we call it aseismic slip or aseismic fault also known as "Creep".

Earthquake prediction is still very tough task for geologists, scientist and others. For future earthquakes prediction and research richer scale, focus, time duration, occurrence period, are also plays a vital role. The size of an earthquake and amount of slip is proportional to the length of the active fault that split during the tremor and the amount of slip. In short we can say that for earthquake prediction research active fault length estimation is required. Therefore, to predict the scale of the earthquake that may happen in the future, it is to estimate the prehistoric fault activity related to that earthquake.

2.2.5 Detection and Mapping of Active Faults

Identification and Mapping of active fault on the premise of geographical, geomorphological and geophysical data, in the region of active tectonics several geomorphological indicator are presented like, atypical river terraces, controlled drainage, Knick points, pull-apart basins, sag ponds, shutter ridges, stream migration, sudden discontinuity of alluvial fans, triangular facets. A USGS image showing surface indicators of active fault. The below figure showing the surface indicator of active fault zone (figure taken from USGS)

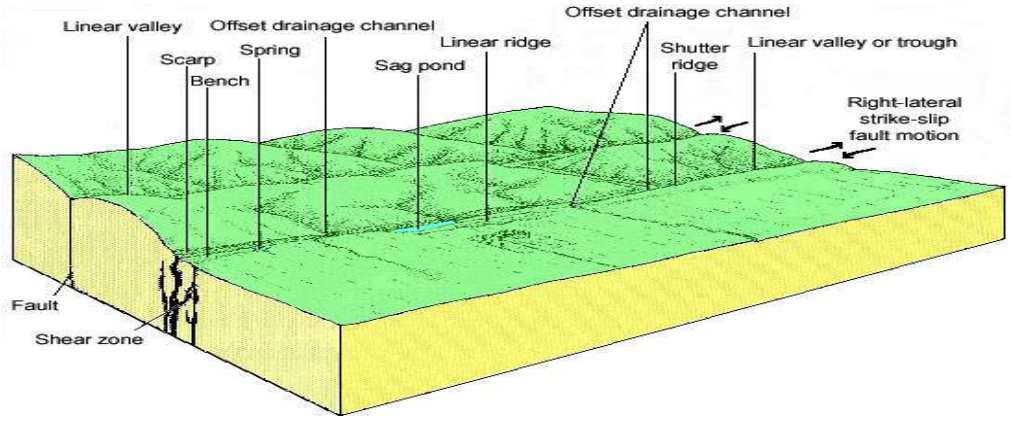

Figure 5 surface Indicator of active fault

1. Geomorphological Approach

Geomorphological approach recognized the recently active breaks in terms of the related geomorphic features like channel offset, channel shift, linear ridge, linear valley, parallel ridges, sag pond, scarps, shutter ridge, spring, terrace and triangulated facet. The fault activity changes the geomorphic landform according to fault movement and fault geometry. The surface indicator of land form clearly marked on remote sensing satellite images/ aerial photo, the Digital elevation model is best explain the active tectonics area on remote sensing and GIS system. Morphotectonic investigation is fundamental tools in geomorphology to classify the relatively active region of area, Lineament study recognize the linear ridge, and parallel ridge and fault line on surface or under the subsurface. The special characteristic of geomorphic land surface are correlated with probable active fault area.

- **Fault Scarp** An abrupt elevation discontinuity on earth surface where one part of fault is steeply uplifted with other one. The movement of fault block can measure by fault scarp and it is the indicator of present tectonics movement or erosion of old fault plane. Eroded/old fault scarp line is mapped with high resolution imagery (Cartosat, Geo-Eye) or LIDAR techniques.

- **Topographic feature :--**Topographic surface where a large/small fault movement is present, marks variations in gradient, the Subtle feature where slight height difference and concealed feature where trace on surface as sag ponds or truncation of old alluvial plain, clearly mapped with High resolution DEM and LIDAR techniques.

- **Geological approach:** ---Rock bed layer examination across the fault displacement area by trenching provides the information of fault activity in past and present time. This investigation support the character of fault, extent of the fault, movement of fault in active fault zone area

- **Geophysical approach**: ---Concealed arrangements of the active faults are investigated by means of Ground penetrating radar (GPR), seismic reflection procedures, sonic prospecting or gravity prospecting, etc. at selected geographical points chosen based on the active fault topography.

2.3 Drainage Analysis

Drainage analysis is useful to identifying the active zone of the area, where plate movement, structure deformation and mass wasting is taking place. Drainage is surficial indicator of underneath geological and geotectonic setting. Drainage anomalies are the abnormalities from the probable drainage in a region. Certain drainage anomalies like deflected drainages, and compressed meanders reflect underlying faults with well-defined morphology. Interpretation of drainage anomalies and the related lineaments/faults provides information for neo-tectonic as well as active tectonic study in the area. Structural or morphotectonic control influences displacement; strike, dip (angles and directions) on landforms due to active tectonics. Sometimes surface expression of structural features is not clear hence includes the stratigraphy of the area; different structural pattern such as joints, faults, folds and bedding planes and lithology.

- **Drainage Anomaly**

Drainage anomaly is part of regional drainage where drainage is controlled by climate, lithology or active tectonics. Drainage anomaly mainly shows the pattern of drainage in not follow the surrounding topographic rules. The drainage anomaly classified based on drainage special characteristic as Rectilinearity of drainage in homogenous medium, local or compress meandering, abrupt change is channel flow and change the river direction in opposite to topographic slope. The below table showing brief details about drainage anomaly types, their morphology and probable cause of anomaly.

Table 1 Details classification scheme of drainage anomalies (Howard, 1967).

Type	Morphology	Cause
Rectilinearity	Long rectilinear segments of streams are anomalies if regional pattern is not rectangular, angular or fault trellis	A fracture, an easily erodable vein or dyke
Local meandering	Abrupt and local appearance of meanders, a straight and simple channel gives two meander-like curves	Structural anomaly dome: subtle upstream change in stream gradient
Compressed meander	Stream pattern of which meanders are normal and in continuous series, squeezed, compressed and incised	Structural anomaly (dome)
Abrupt and localised braiding	Abrupt and localised braiding. It could be indicated by variations in drainage density	Braiding indicates inability of a stream to transport its bed load
Flaring in valley	Local widening or narrowing of valleys or channel	Local structure, shallow upwarp

Anomalous ponds, marshes	Isolated ponds and marshes	Subsidence or uplift
Anomalous breadth of levees	Abandoned channels are locally narrow	Subsidence, levees wider
Flying levees	Levees locally preserved	Subsidence or buried structural features
Anomalous curves and turns	Varieties and legion	Piracy, Domal upwarp and strike slip fault

Drainage always follow the easiest path on a terrain until it connects with other streams in the drainage system. The behavior of drainage pattern influenced by different geologic structures underneath as well as terrain movement. Any abnormal deviation from the normal stream defines drainage distortion such as abrupt change in drainage direction, existence of compressed meanders and abrupt termination of drainage.

2.4 Ground penetrating Radar (GPR)

2.4.1 Principles

Ground Penetrating Radar (GPR) is a high-resolution geophysical technique used to study the shallow subsurface. It measures the reflections of an electromagnetic (EM) pulse penetrating the subsurface materials in a frequency range generally between 20 MHz and 1 GHz. Changes in dielectric properties are responsible for the EM wave reflections and diffractions. GPR traces are collected and showed in a "radargram", where the amplitude of EM signals is recorded as a function of the distance (trace position) and the two-way travel time. The GPR data, after the application of a suitable processing flow, can be used to obtain a reliable subsurface image and to extract several physical parameters (e.g. EM wave velocity, electrical permittivity, EM intrinsic attenuation), that can be finally interpreted according to the geologic data available for the survey site and the preliminary purposes (Jol, 2009)

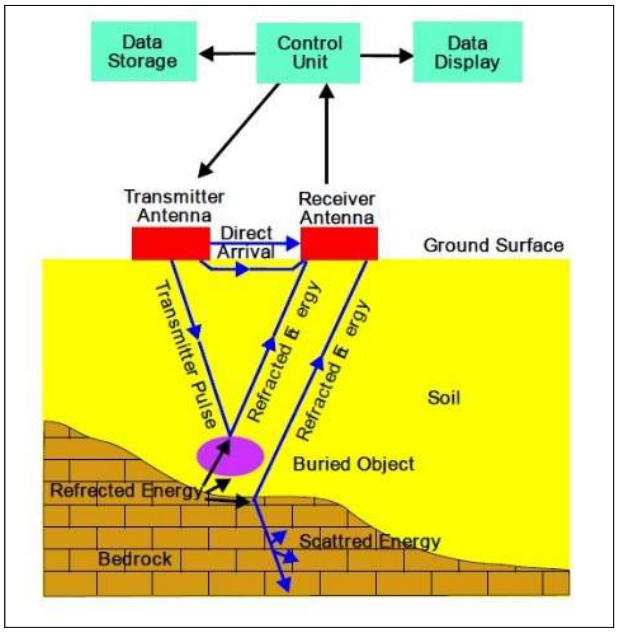

Figure 6 GPR Principle of Operation (from ASTM 6432)

Electrical properties of some geologic materials

Ground penetrating radar governed by dielectric constant (permittivity), Magnetic permeability and conductivity of sub-surface layers. In general case the dielectric permittivity is major properties of GPR and its control the penetration depth and resolution of radar profiles. Typical electrical properties of some common geological materials at low frequency antenna, Table from (Neal , 2004)

Table 2 Electrical properties of common geological materials.

Medium	Relative dielectric permittivity (Er)	Electromagnetic-wave velocity (m ns^{-1})	Conductivity (mSm^{-1})	Attenuation (dB m^{-1})
Air	1	0.3	0	0
Fresh water	80	0.03	0.5	0.1
Sea water	80	0.01	30,000	1000
Unsaturated sand	2.55 – 7.5	0.1 – 0.2	0.01	0.01– 0.14
Saturated sand	20 – 31.6	0.05 – 0.08	0.1 – 1	0.03– 0.5
Unsaturated sand and gravel	3.5 – 6.5	0.09 – 0.13	0.007 – 0.06	0.01– 0.1
Saturated sand and gravel	15.5 – 17.5	0.06	0.7 – 9	0.03– 0.5
Unsaturated silt	2.5 – 5	0.09 – 0.12	1 – 100	1 –300a
Saturated silt	22 – 30	0.05 – 0.07	100	1 –300a
Unsaturated clay	2.5 – 5	0.09 – 0.12	2 – 20	0.28– 300a
Saturated clay	15 – 40	0.05 – 0.07	20 – 1000	0.28– 300a
Unsaturated till	7.4 – 21.1	0.1 – 0.12*	2.5 – 10	b
Saturated till	24 – 34	0.1 – 0.12*	2 – 5	b
Freshwater peat	57 – 80	0.03 – 0.06	< 40	0.3
Bedrock	4 – 6	0.12 – 0.13	10 -5 – 40	7x10-6 – 24

From Neal

[a] Unsaturated and saturated values not differentiated (Neal , 2004)

[b] Values not available.

"Reflection of the energy occurs when a change in the properties of the subsurface occurs. Given two neighboring layers with different properties, which are example by different relative electric permittivity's (ε_{r1} and ε_{r2}), a reflection coefficient (R) can be calculated thus (Reynolds, 1997):

$$R = \frac{\sqrt{\varepsilon_{r2}} - \sqrt{\varepsilon_{r1}}}{\sqrt{\varepsilon_{r2}} + \sqrt{\varepsilon_{r1}}}$$

The ε_{r1} is the dielectric constant of medium 1 and is the ε_{r2} dielectric constant of medium 2. R is reflection coefficient. The amount of energy reflected increase as the difference between

dielectric constant increases. The relative permittivity within sediments is controlled by the moisture content, lithology, sediment packing or sorting. Therefore, lithological changes, deformation structure or water table should be detected by GPR (Neal , 2004). Reflection coefficient will range between +1 and -1, the polarity of the reflected wave is indicated by the sign.

2.4.2 Signal Types

EM wave affect the subsurface materials depending on the size, orientation, and chemical and physical properties of geological deposits. The signal patterns of EM wave fall under one of two basic categories such as planar reflections, produced at transitions between deposits and/or features and point source reflections, produced by discrete point targets. Signals can also be distinguished by change in amplitude indicating changes in subsurface materials.

- **Planar Reflections** created from horizontal, rectilinear and inclined boundary of subsurface material, such as different geological strata, water table, enforced different material, fracture/fault line (inclined), the planner reflection appears as horizontal or some dipping line in radargram profiles and its main application to measure the depth, size, shape and orientation of underground boundaries and discontinuities.

- **Point Source or Hyperbolas reflections** generated from point or non-planner objects like metallic/ nonmetallic pipe, distinct objects, spatially-limited matters, cavities, tunnels, rocks boulders. The primary condition for acquiring of hyperbolas in GPR profiling must be crossed at right angle in the case of linear feature as pipe, tunnel, etc. GPR electromagnetic wave shaped look like form of cone, the emitted wave goes forward ward with subsurface depth and after collision from point source or pipe it gives hyperbola reflection. Basically the energy are not directly record below on antenna in the case of point or pipe reflection when its record the underneath the antenna at a greater depth due to slanted communication of the EM waves. The actually position of point or pipe (across the profile) is top of the hyperbola reflections.

- **Amplitude changes refection** generated where the subsurface materials, have strongly different from each other due to physical and chemical properties and thus difference in reflection coefficient.

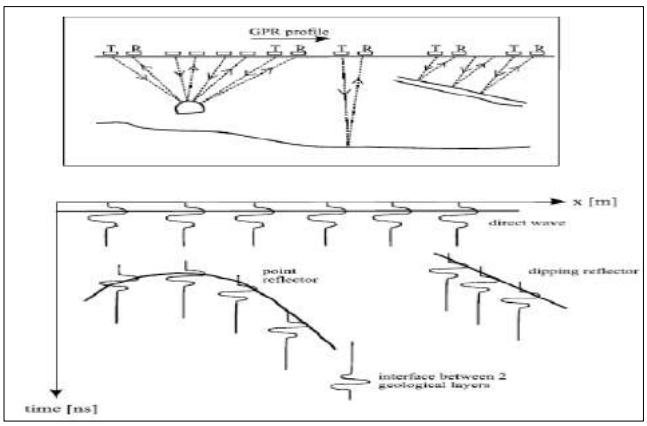

Figure 7 Principle of GPR constant-offset survey (Pernito,

2.4.3 Survey Techniques

GPR is a non-destructive, geophysical method to collect the information about subsurface material within the maximum limit of 50 m. Thus a survey techniques have significant role in the data acquisition or resolution of the radar data. Appropriate radar antenna frequency and survey plan gives the better penetration as well as better resolution. According to Objective of GPR data research planning and design of survey should be initiate, several factors are considered during survey such as geology, topography and size, shape and orientation of the target. The GPR technique is very sensitive to surrounding as well as operational noise, so source of noise also be considered. Efficient GPR data acquisition depends on proper and detailed planning of survey, different techniques to be considered while surveying are as follows:

A. **Depth of Penetration:--**The penetration depth of GPR signals is defined by depletion affected by scattering, geometric dispersion, and dielectric permittivity, planning a beneficial GPR survey is the measurement of expected penetration depth of target characteristic or avoid another unwanted target.

B. ***EM Property of material Contrast:*** -- EM property is main fundamental elements in preparation of GPR survey is the purpose of whether or not there is satisfactory difference between target object and surrounding geological unit. In case of geological application its main concern about demarcate the two geological unit or fault/fracture plane material.

C. **Selection of the Approach: --** The main goal of the selection of specific antenna and different mode of survey according antenna separation. In general two mode are use, a) Radar antenna drag along survey line b) Radar antenna (Tx and Tr)are fixed are acquiring the specific point information along the survey line.

D. **Survey Design:--**Location and area of Survey site is beneficial to visit survey site and design the strategy before the GPR operation, if visiting the survey site is not possible then you can make a rough draw of survey lines with the help of aerial photo/satellite image/ topographic map. The elevation data should be obtained along survey line or avoid the larger elevation difference. The area of survey location must be greater than that concern area so make an idea about underground geological material. The survey line should be straight, perpendicular across the area of interested, line space must be adjusted according to the shape, size or orientation of target.

E. ***Survey Implementation:***

- Calibration and Standardization is needed for operational check of equipment and regulate with survey site environment.

- Survey Lines- always try to take a survey must be a straight line. Place position marks at equal intervals along the survey line using paint marker and tape. New advance technique Total station survey, DGPS gives an accurate scan line information with accurate height variation data.

- On-site Check of the Plan: The initial measurement of radar profile can gives the information about S/N ratio and electromagnetic properties of material. If on site result is not according to the objective then we can shift with surrounding nearest area which matching with our Goal.

2.4.4 Data Processing / Analysis

In maximum radar survey, the preliminary result of radar data show with radargram in real time scanning, but the post processing is required for appropriate position of radargram, removal of surrounding noise and operation noise. Different operation like spatial domain filters, time domain filters, migrations are applied in radar data for correction of radar data.

A variety of filtering methods may be used to remove or minimize noise in GPR data. In back ground removal techniques by averaging of all radar scan in data set being subtracted by each scene. Medium gradient filters are used for removing the noise of surrounding radio frequency from different EM source. Topographic correction is technique where elevation variation presented in radar data may be corrected by GPS data or total station data acquired from time of GPR acquisition.

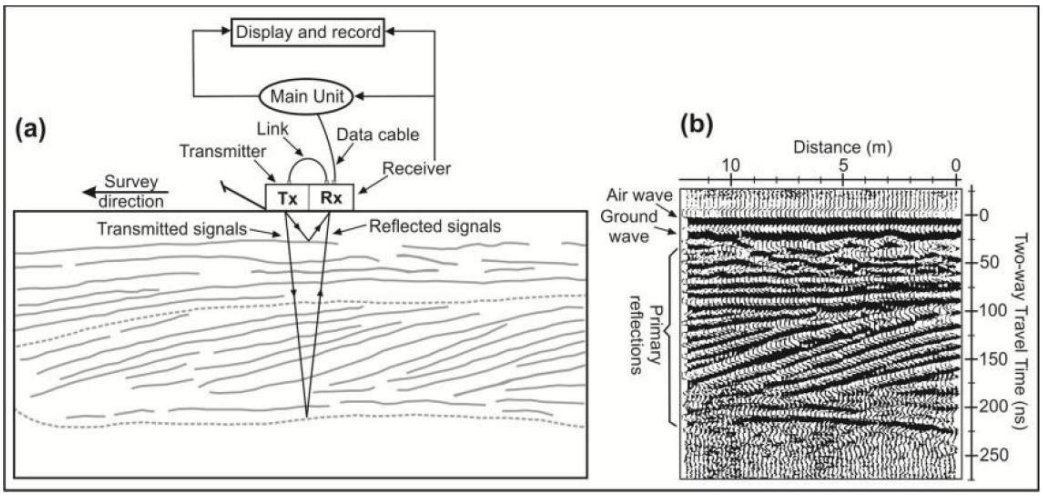

Figure 8 GPR data acquisition and the resulting radar profile in wiggle mode

Above Figure Showing, (a) The schematic GPR acquisition process showing radar wave penetration (b) GPR radargram profile showing bedding plane in wiggle mode. (Neal , 2004).

2.4.5 Applications

The GPR is subsurface mapping techniques which can applicable in field of archeology, fault and fracture mapping, sedimentology, forestry (root estimation), glaciology, costal mapping, lithological mapping, karst investigation, engineering foundation mapping, and planetary mapping (Kaguya project, 2007).

The use of GPR as a geophysical method of site investigation has several beneficial advantages compared to other subsurface sensing technologies such as

- Non-destructive nature;
- Its ability to maximise research efficiency and minimise the cost;
- Its capability to cover large areas quickly;
- The capability in detecting both metallic and non-metallic targets

In comparison to other subsurface sensing technologies, GPR has the potential to increase research efficiency by conducting surveys quickly at relatively low cost as well as covering larger areas. The antennas of GPR itself may be pulled by hand or with a vehicle which can produce considerable data/unit time that makes the GPR measurements relatively easy to make.

2.4.6 Limitations

Every geophysical instrument have some drawback, so GPR has some limitation factors; GPR techniques mainly site based and penetration depth and its resolution depends upon physical and chemical properties of subsurface materials. It ideal penetration depth is maximum 30m in geological terrain.

- Sensitivity: --- GPR techniques is easily affected by surrounding undesirable factors (Mobile phones, trees, large building, and vehicles) in the case of unshielded antenna although Shielded antenna are not affected by surface features but it has also some unwanted disturbance by building foundation, large tree roots, underground electric pipes etc.
- Material Properties Contrast: --- subsurface materials have different reflection coefficient which depends upon amplitude of emitted and received radar signals, angle of incident, and incident polarization. Different subsurface boundary mark by sufficient velocity of radar wave.
- Attenuation: --- radar wave attenuation is produced by the result of dielectric permittivity, magnetic properties of soil (Clay or Iron rich) and geometric dispersion of signals. In dielectric permittivity reductions because of rotational polarization of the water particle and chemical charge relocation procedures on the surface of clay materials. Free ions in clay sediments and some Electrical conductive material reduce the radar signal strength by transforming the electromagnetic wave energy into thermal energy. Scattering is main reason in the case of in-homogeneous material where radar wavelength match with grain size of material.

2.5 SAR Interferometry

2.5.1 Interferometric Synthetic aperture radar (InSAR)

Interferometry Synthetic Aperture Radar (InSAR) is active remote sensing techniques that can calculate the ground movement rate (horizontally, vertically) by measuring the two phase change of same pixel of earth surface. Interferometry techniques can be applied in the measurement of earth surface change in millimeter to centimeter level.

2.5.2 ScanSAR Interferometry

ScanSAR mode has a great advantage to achieve a wide coverage by rotating the antenna into different angle. Strip mode data has high resolution and high S/N ration but swath is only 70*70 km however FBS mode has also the capability to measure the large crustal movement by joining the fringe pattern of surrounding datasets, due to phase discontinuity and different data acquisition time the analysis of large crustal movement is not effectively helpful. In ScanSAR data interferometry the larger swath width (350 km*350 km and 100m moderate resolution) gives better perspective of large scale crustal movement due to earthquake and active plate motion.

(Jiang, et al., 2008) have tried to achieve the wide range crustal movement using ScanSAR interferometry techniques on ENVISAT wide beam data. The main focus of their work to identify the large scale crustal deformation along the Xianshuihe active fault. In their study six WS-WS data of ENVISAT HH & HV polarization has been taken and processed by GAMMA software. Initially the activity of fault is recorded as a fringe in their WS interferometry result, although due to atmospheric noise, orbit uncertainty height error, the result is showing much larger than fault movement. A phase stacking process applied for removing those noises and got the result approx. 5~10 mm/yr. across the Xianshuihe fault and 10~15 mm/yr. across the GarZe-Yushu fault.

(Liang, et al., 2009) (Cui, et al., 2010) have applied the SCANSAR interferometry with ALOS PALSAR WB1 data ithe areaea of Wenchuan earthquake china, they focused on Full aperture algorithm, strip map algorithm (modified) and to fill the burst echoes and create the SLC image for each beam. In DInSAR processing the single beam (Master & Slave) processed like strip map mode data without any relation with another beam after processing of all beam then it mosaicked together to form the full Wide scene. SRTM 90 m DEM were used for removing the topographic Noise phase. The result obtained for Wenchuan earthquake showing some movement and large scale deformation in the study area. The (Cui, et al., 2010) rework with PUMSIP software and obtained the result as Differential interferogram unwrapped phase deformation map in the LOS direction approx. 11.8 cm. The obtained ALOS WB1 L-band result map is better than ENVISAT ASAR ‘C’ band data result.

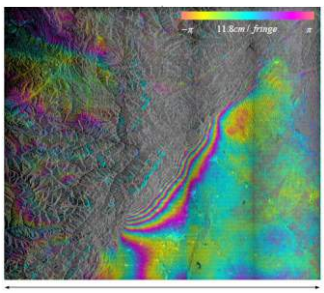

Figure 9 Deformation Map of Wenchuan Earthquake **(Liang, et al., 2009)**

(Liang, et al., 2010) attempted to generate the SCANSAR (WB1) with High resolution Fine beam dual polarization (FBD) images in part of Iran area. They used a fourth beam of WB1 data and FBD for processing, strip mode processing step was used for D-Interferometry. In this study no crustal study movement was found, however the generation of DEM and analysis of interferometry show the inability of WB1-FBD interferometry in high relief area. They proved that the different mode ScanSAR and FBD data processing.

(Caijun, et al., 2011) have proposed the interferometry process with atmospheric correction by using ENVISAT ASAR wide-swath data processing with MODIS data in the Wenchuan earthquake deformation area. They used ROI_PAC software for Interferometry processing and Zenith wet delay algorithm for noise correction. The obtained result was not satisfactory in comparison from the GPS movement result. (Caijun, et al., 2011) Claimed that the clarity of the deformation fringe of ENVISAT A-ASAR data result is better than ALOS WB1 result, because the correction of water vapor noise with MODIS data. The expected result was not achieved due to incoherence however the ScanSAR mode has great capability to measure the active crust or coseismal activity.

(Miyawaki, et al., 2011) (Miyawaki & Kimura, 2013) have analysed the large scale crustal movement due to earthquake in Chile region and Wenchuan, china by using ALOS/PALSAR wide beam data. The prime focus of this study was to prove the crustal deformation and its relation with huge earthquake using wide beam data, because the area of large movement can't not correctly measure by small scale 70*70 km swath of fine beam data. After processing the all master beam corresponding to slave bema obtained the good result in both study area. (Miyawaki & Kimura, 2013) also attempted the Tohoku earthquake 2011 in Japan (Mw 9.0) good result was achieved from Tohoku earthquake deformed area.

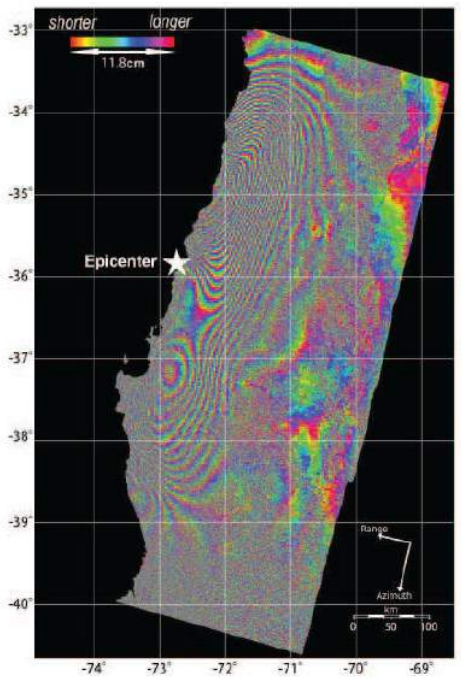

Figure 11 Chilli earthquake deformation map, (Miyawaki, et al., 2011)

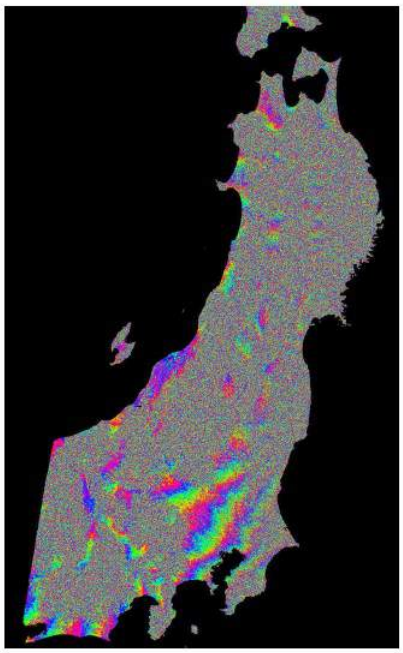

Figure 10 Tohoku, japan earthquake deformation map **(Miyawaki & Kimura, 2013)**

3 STUDY AREA AND MATERIALS / DATA USED

3.1 Study area

The boundary between the Siwalik and the Indo Gangetic Plain is a discontinuous zone of reverse faulting called the Himalayan Thrust (HFT). HFT is generally marked by the contact of the bedrock Siwalik Group and Quaternary alluvium. Locally, the HFT is expressed in young alluvium as relatively short and discontinuous range fault scarps that cut Quaternary fluvial terraces and alluvial fans.

3.1.1 Location

The area under study covers a major part of Uttarakhand and some portion of Uttar Pradesh, Haryana, Himachal Pradesh, Chandigarh and Punjab within latitudes 28°41'N - 31°40'N and longitude 76°36' E- 79°30'E. The present study is confined only to HFT piedmont plain areas.

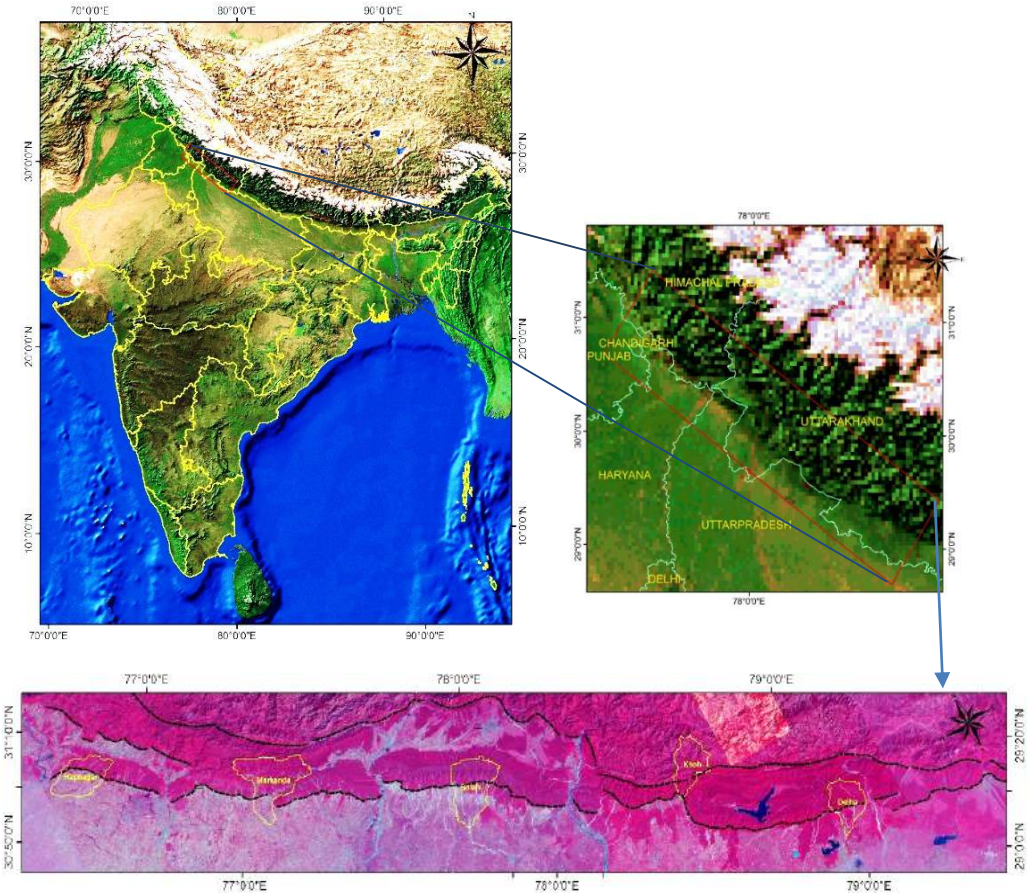

Figure 12 Study area

3.1.2 Geologic and Tectonic setting

The study area is part of Himalaya known as Kumaun Himalaya, which boundary is marked between Kali River and Sutlej River from east to west respectively. The study area essentially lies within Himalayan; piedmont region, sub-Himalaya and a part of lesser Himalaya. The lesser Himalayan bed rock is clearly marked boundary is known as Main Boundary thrust, the sub-Himalayan region mainly formed of eroded sediments from lesser Himalaya. The upper and middle Siwalik range is not presented toward east of the Himalaya, the bed rock of upper Siwalik (Boulder and Conglomerate) is tectonically deformed, in Dun area where bed rocks (gravels & boulder) are younger deposited from Siwalik and lesser Himalaya erosion (Kothyari, et al., 2010) (Nakata, 1972)

In the Himalayan region the neotectonic activity, active fault indication related to thrust movement are confined to some section. The MCT is supposed to inactive excluding some re-activation reported in central Nepal Himalayan region. The MBT showing the Neotectonics activity in some region. According to Gansser and Valdiya the MBT and MCT mainly showing Cenozoic shortening along whole stretch of Himalayan region. But in the Himalayan frontal thrust has been clearly show the uplifting of Holocene and recent deposited bed, active faulting and its marks the zone of active deformation between rigid moving Indian plate and Himalayan foot hill zone.

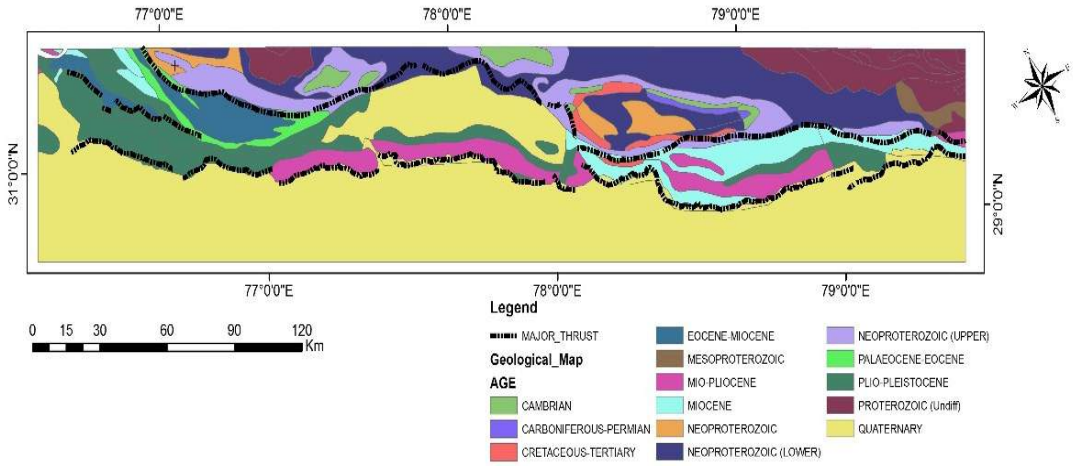

Figure 13 Geological Map of Study area (Modified from GSI & Valdiya)

3.2 Data used

This section provides information about the data and data formats, which used in this study.

In this study the following data have been used

Table 3 Description of Data

Type	Date/ Year	Quantity	Resolution/ Scale	Purpose
Satellite Data (Optical and Microwave)				
CARTOSAT-1 stereo data	2009, 2010, 2011	18	2.5 m	High resolution digital elevation model generation (DEM) and Ortho-photo, Topographic analysis.
LISS-III	2007,2008,2009,2010	22	23.5 m	Generation of mosaic data and mapping of morphological parameter.
LANDSAT MSS/TM/ ETM+ & OLI	1980 – 2014 (Temporal Data)	30	30 m MSS/ 15 m PAN	Mapping and Drainage analysis
RISAT (MRS)	2013	8	21-23 m (Az) / 8m (Slant)	Regional Structure / Lineament mapping
Radarsat-2 (WB)	2013	1	100 m	Regional Structure / Lineament mapping
ALOS PALSAR (SCAN)	2008, 2009, 2010	12	100 m	Crustal deformation measurement and Structure and lineament mapping
Topographic Data				
CartoDEM Version-3 R1	NRSC	------	30 m/ 10m	Topographic analysis
SRTM DEM	USGS		30 m	Topographic analysis, Topographic phase removal in D-InSAR processing.
Ancillary Data				
DGPS Survey Points	2014, 2015	42 Points	Centimeter	GCP collection for High accurate DEM and Ortho-photo generation
Toposheet	1957-1976		1:50,000	Mapping and SPOT Height
Seismo-tectonic Atlas	2000		1:1,000,000	Fault and Lineament mapping
Geology Map	1998	1	1:2,000,000	Mapping
Geomorphology Map	2009	1	1:2,000,000	Mapping
GPR Survey	2014, 2015	10location, 30Profiles	Centimeter	Mapping and validating the subsurface structure.

3.2.1 Remote Sensing Satellite data

In this study different satellite images that were used for the generation of drainage anomaly map. Temporal dataset gives the information about drainage migration and identifying the activity of geomorphic landforms. Cartosat-1 data used for generation of highly accurate DEM for topographic analysis. Microwave data especially (RISAT AND RADARSAT-2 data) ScanSAR mode helps the regional mapping of structure and lineaments.

3.2.2 DEM Data

High accurate DEM data is generated from Cartosat-1 (Stereo pair) with accuracy of 10 m for terrain analysis in specific basin. CartoDEM Version- R1, 30 m from Bhuvan, NRSC and

SRTM (Shuttle Radar Topographic Mission) DEM with 30m X 30m spatial resolution has been used for topographic phase compensation and differential Interferogram generation.

3.2.3 Software Tools

SOFTWARE	PURPOSE
ArcGIS 10.2	Analysis of spatial data, Topography Mapping and Topographic analysis.
ENVI 5.1	Digital Image processing and Topographic analysis.
ERDAS 14	DEM generation, Digital Image processing and Topographic analysis.
GAMMA	Microwave Data processing from L0 (Raw Data).
GRED HD	GPR data processing, Visualizing and Interpretation.
K2 fast WAVE	GPR data acquisition.
Microsoft Office	Report writing
Quantum GIS	WMS layer and mapping
SARSCPE 5.1	RADAR Data processing.
Sentinel- 1	RADAR Data processing.
Trimble Business center	DGPS data processing.

3.2.4 Field Equipment

- Handheld GPS Device –Garmin (Model: Oregon 550)
- IDS GPR with 100 and 40 MHz antenna.
- Trimble R7 and R9 GNNS receiver.
- NIKON 16 Megapixel Camera.
- Brunton compass.
- Measuring Tape.

4 METHODOLOGY

The present work is divided into three broad research objectives, geomorphic analysis, ground penetrating radar profiling, and microwave data analysis.

Broadly the following methodologies were adopted in the present study is as follows

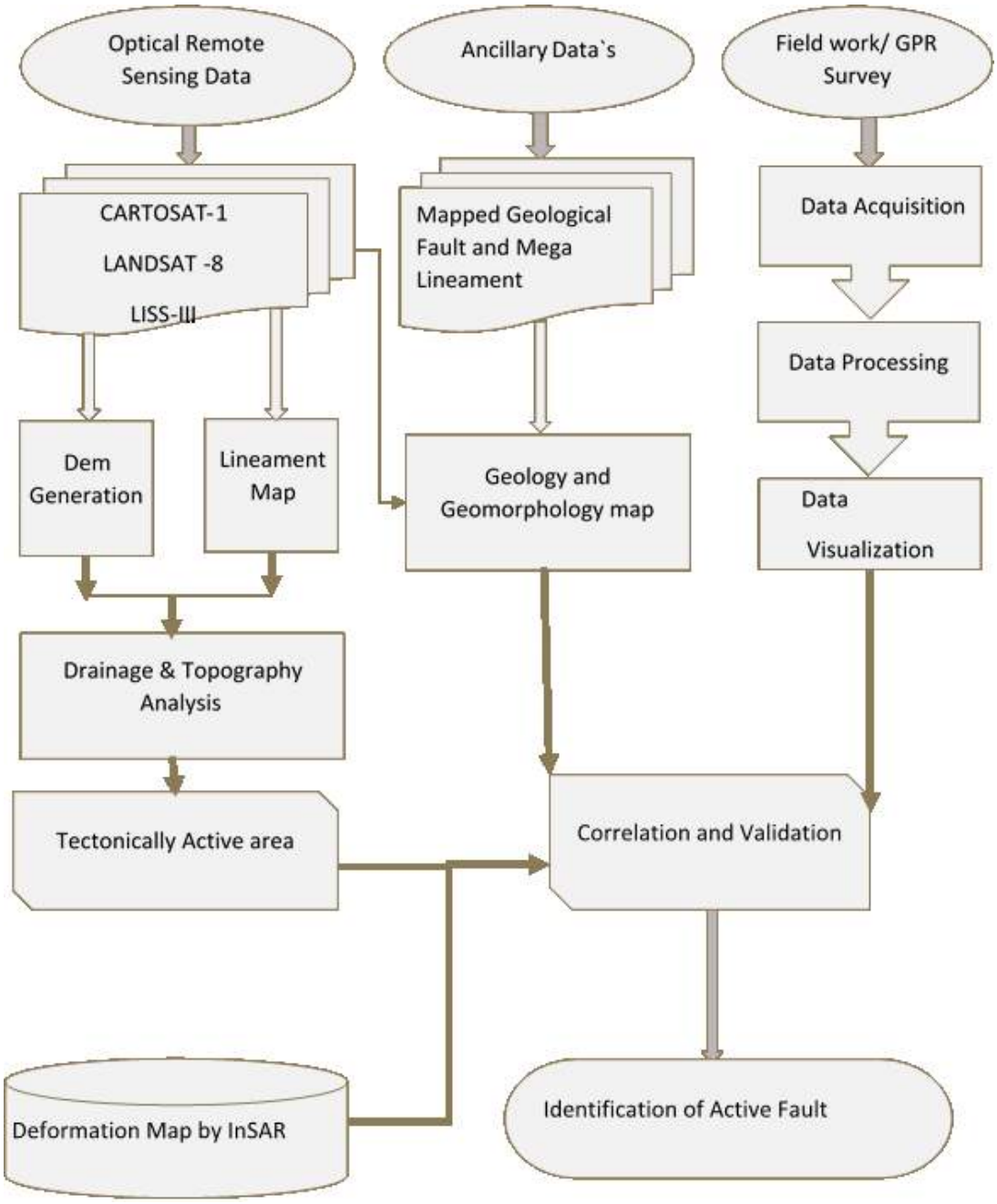

Figure 14 Overall methodology Flow Diagram

4.1 DEM generation

The combined use of remotely sensed data and DEMs can be useful for investigating the morphology of an active tectonic region. DEMs derived from high-resolution imagery will improve our understanding of active tectonic surface ruptures in complex tectonic settings. Remote sensing techniques (e.g. DEMs) have potential for picking up displaced geomorphic surfaces, river terraces, drainage channels, alluvial fans, lineaments and topographic ridges which are potential signatures of the appearance of active tectonics.

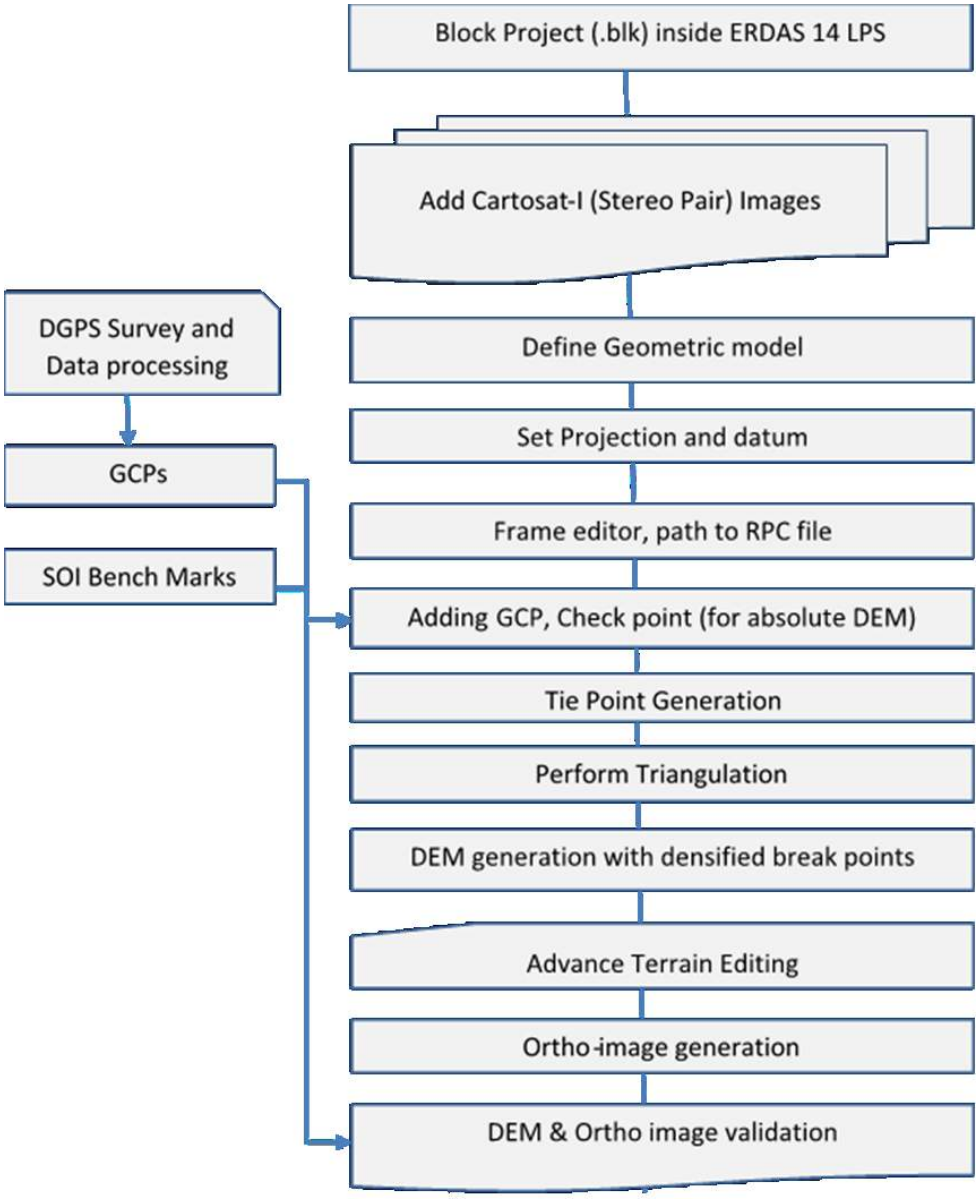

Figure 15 Flow chart of DEM generation with CARTOSAT-1 stereo data

4.1.1 Ground control Point collection using Differential GPS

Ground control points collected in the area of Chandigarh, kala-amb Solani and Ramnagar. In this process, well distributed and accurate ground control points (GCP) were collected using Dual frequency Trimble R7 and R9 GNNS Differential GPS instrument in campaign mode for a duration of minimum one hour for each. Post processing were carried out using Trimble Business center v 2.8 software.

Figure 16 Ground control Survey base station and Rover

Figure: -- (A) DGPS base station (Trimble R7 & R9 GNNS receiver) at SASE guest house, Chandigarh. (B) Rover at Markanda basin, (C) Rover

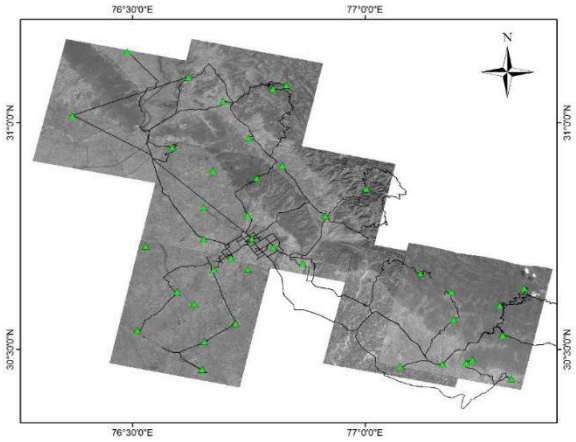

Figure 18 GCP locations using DGPS for DEM generation.

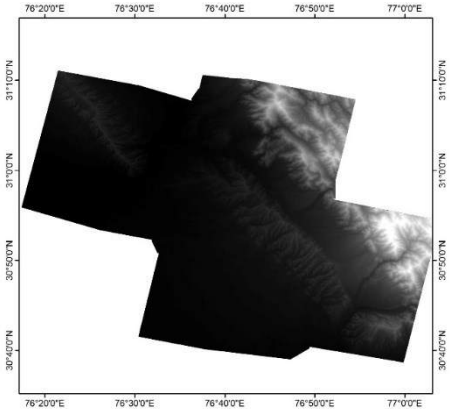

Figure 17 High Resolution DEM from Cartosat-1 Stereo Imagery

To generate digital elevation model ERDAS 14 (Photogrammetry tools) have been used and the steps followed as below

- Create a new block file(*.blk) by defining geometric model category i.e. Rational Function and Geometric model i.e. Cartosat RPC, define the reference co-ordinate system in Horizontal (Projection type-UTM, Spheroid/Datum-WGS 84) and Vertical (Spheroid/Datum-WGS84, Elevation Units-meters, Elevation Type-Height).

- In add frame under edit category, define the Path of both the bands of Cartosat stereo pair.
- In frame editor define the path of RPC (Rational Polynomial Coefficient) file.
- Compute the Pyramid layer of both the bands by clicking on Compute Pyramid Layer Category.
- Select the Classical Point measurement tool under the category point measurement.
- Select the GCP point (DGPS & SOI Bench mark) as a control point and minimum 2 GCP should be as a Check point for accuracy measurement.
- Selecting the same point on Band F image and then we used manual input the tie point and auto triangulation box for auto tie point generation. We selected more than 100 tie points.
- Run the triangulation process
- Total RMSE should not more than half pixel while using second order polynomial.
- Generate the orthoimage after DEM generation.
- Validation with check point and SOI Topo-sheet Spot height.

4.2 Topography Analysis by Profiling

Topography is the control by climate, lithology and active tectonics, but in the Himalayan foot hill region where alluvial fan deposit clearly shows that the landform is control by underneath geological setting and active tectonics. Topographic profile is a line which draw on elevation data (contour or DEM) which gives the information of height along the line, the height information reveals the landform shape size and its geometry. Topographic profiling is 2-D representation of height data for evaluation of landform and its associated processes. A tectonically active region modified the landform according to structural and geological setting of that area which can identify by topographic analysis. Topographic analysis is essential to define the active zone of area by measuring abrupt elevation difference like fault scarp etc. For evaluation of topography profile, five basin were selected in Himalayan foot fill region. Digital Elevation Models (DEMs) have been used in topographic analysis to understand the relationship between tectonic activity, associated landscape features and evolution. The topographic analysis was performed using highly accurate 10 m resolution DEM that was constructed using Ground control points (DGPS points and SOI Bench Marks).The first step in topographic analysis, profile drawn in Himalayan piedmont area after HFT in five basin namely Dhela, Khoh, Solani Markanda and RupNagar Basin. Elevation difference and elevation gradient, which convey signals of subsurface lithology, climate condition and of possible tectonic movements, were analysed with ERDAS (Spatial profile tool) and ArcGIS software (Spatial analyst tool)

4.3 Drainage Analysis

The methodology for identifying drainage anomaly and drainage migration.

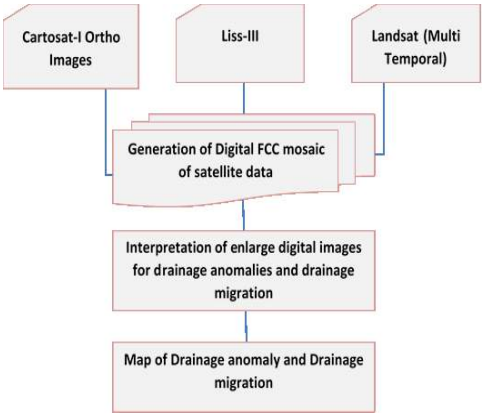

Figure 19 Methodology flow chart for drainage analysis.

- **Analysis of satellite Images**

Different types of satellite images were used in this study, which have different resolution and optical properties. The variation in the resolution of the selected images would cause uncertainty in the analysis and hence resampled to same resolution. The processed images are Cartosat-1(2.5 m) orthoimages, LISS-III (23.5 m), Landsat TM/ETM+ and 8 (Pan 15m and MSS 30 m). Different digital image enhancement technique like radiometric correction, histogram equalization and other preprocessing were done before mosaicking. Co-registration with multi-temporal satellite data were performed for drainage migration analysis.

a. Drainage Anomaly Analysis

Drainage is primary visible factors that easily influenced by climate, lithology and active tectonics. In the tectonically active area where soft soil deposition in the form of alluvial fan clearly show the tectonic activity. Drainage anomaly reveals the subsurface structural and geological setting of the area, the information given as a form of drainage anomaly suggest that the deformation pattern and its location. We investigated in the Himalayan foot hill zone for drainage anomaly and concentrated on five major basin from east to west named Dhela Basin, Uk. Khoh Basin, UK, Solani basin, Markanda basin and Rup nagar basin. The methodology used to determine the presence of an anomaly in the flowing direction of the drainage network is shown in above flow chart. We constructed a database of 141 anomalous reaches along more than 10 rivers including their tributary. Each anomaly is believed to be evidence of the activity of a sub-surface structure. Some examples are shown in Table 4.

Table 4 Drainage anomalies recognized in the study area, their location

Id	Latitude	Longitude	Drainage Anomaly	Location Name
1	29.09024614	29.09024614	Right Angled bend	Govind nagar
2	29.15157821	29.15157821	Localized Braiding	Rooppur
3	28.87602153	28.87602153	Rectilinearity	Anjania
4	28.75059048	28.75059048	Compressed Meandering	Itavadhura
5	29.27361524	29.27361524	Zone of Distributary bifurcation	kathgodam
6	29.20941851	29.20941851	Deflection of Stream Channel	Indira nagar

a. Drainage Migration/ Shift /Capturing Analysis

The drainage shift or migration term are used where one river can change their path abruptly or slowly. Drainage shifting is generally control by subsurface structure. The paleochannel is prime indicator of drainage shift in area, its shows the past position of river flow and changing location into another location control by structure setting.

The analysis of river shift/migration is made with the combination of temporal satellite data, literature data and geomorphological data from the basin and its margin. Most of the available cases of river shifts in Himalayan foot hill basin are characterized by the migration of a deflection point of the river along structural trends and drainage follow along the fault. For this drainage shift analysis we build a data base with location and associate reason for drainage migration. Some examples are shown in table.

Table 5 Drainage migration with associate anomaly

Drainage Migration with Associated Anomaly			
Sr. No.	Latitude	Latitude	Related Anomaly
1	28.86352527	79.50078104	RIGHT ANGLED BEND+ SOUTHEAST SHIFT
2	29.1947182	79.61354018	ZONE OF DIVERGENCE SHIFTED NORTHWARDS
3	29.14865101	79.71071847	STREAM DIRECTION SHIFTS WESTWARDS
4	30.42514188	77.58176849	POINT OF CONFLUENCE SHIFTS NORTHWARDS
5	30.15013722	77.88474395	DIVERGING CHANNELS APPEARS ON LEFT FLANCK
6	29.15700914	79.61513512	POINT OF CONFLUENCE RETREATED UPSTREAM

4.4 Ground Penetrating Radar (GPR)

Ground Penetrating Radar, (GPR) or Georadar is a high resolution geophysical measurement method that allows the investigation of the shallow subsurface. A GPR antenna is used to the detection and recording of changes in dielectric properties in the shallow subsurface. The radar signal is transmitted from one antenna and travels down through subsurface where a receiving antenna records the returning energy as a function of travel time since the transmission of the signals used to generate an image of the subsurface (Neal, 2004). Ideally, GPR may provide high-resolution images of the subsurface over a depth range of several meters to, extremely, 50 m. However, the quality of the data and the depth of penetration strongly depend on the dielectric properties of the investigated material and the frequency range of the antennae used.

The objective of this present study is to identify and characterize active fault where geomorphological expression of a fault is present in the topography and test the applicability of GPR imaging across very recent surface ruptures and determine the exact position and characteristic of the active fault (location & dip) in shallow depth.

The method used for IDS GPR datasets consists three phase which include, First correction of data, background noise removal and secondly filtering the data with different domain and give Auto and manual gain and finally visualization and interpretation of data.

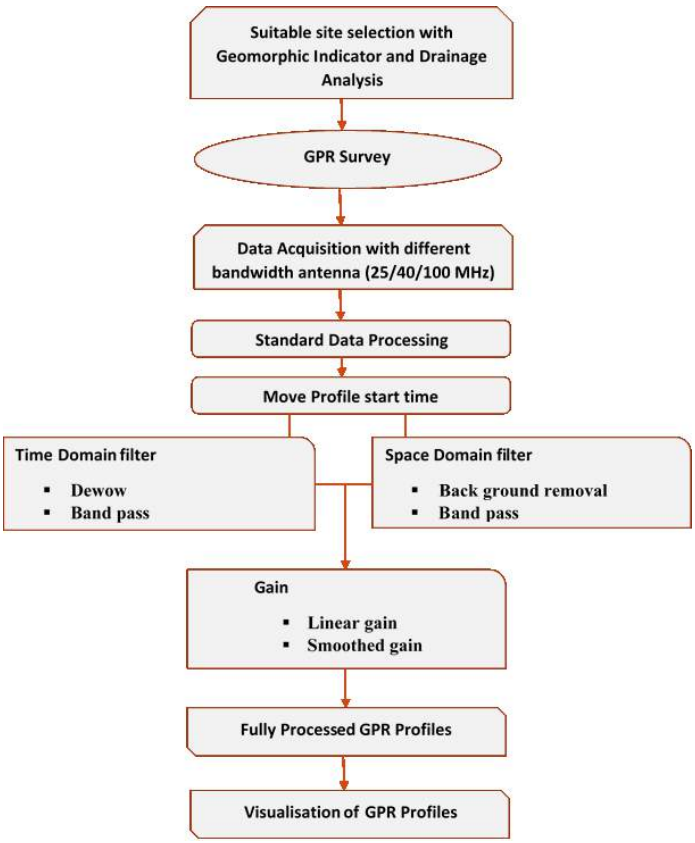

Figure 20 GPR Data Processing Flow Chart (IDS)

Above block diagram describes the processing flow used for analysing GPR data using GRED HD software. The basic descriptions of each step are as follows

- **The Move start time** (Time-zero correction):-- correction of start time to match with surface position;
- **The Move Profile start time:** -- command align a radar section according to the move start time calculated for each sweep.
- **Back Ground removal:** -- removal and correction of bad/poor data and sorting of data files
- **Band pass filtering:** -- 1D and 2D filtering to improve SNR and visual quality;
- **Linear Gain:** -- The Linear gain command is used to apply a filtering algorithm of the power equalization along a sweep to a selected radar map on the basis of an estimated linear attenuation.
- **Smooth Gain:** -- The Smoothed gain filtering algorithm is used to equalize the power along a sweep for a moving window estimated linear attenuation.

- **User Defined Gain:** -- This applies a filtering algorithm used for applying your own customized gain curve.
- **Migration:** -- The migration function helps in rearranging the true position of steeply dipping reflections and hyperbolic diffractions. Correction of the survey geometry and spatial distribution of energy effects.
- **Macro:** -- command is used for processing radar data and for applying a preset sequence of filters.

4.4.1 GPR Hardware (Instrumental Configuration)

This section describes the field experiments which will be carried out of our test sites in the locality of HFT. Here, different GPR antenna techniques will be applied and measurements will be recorded for comparison.

Equipment used for GPR survey

The instrument used in the present study is IDS (INGENERIA DEI SISTEMI S.p. A). In IDS GPR system, there was two types of antenna; for this project, the 100 MHz (Shielded), & 40 MHz (unshielded) antenna system used. There was following items and their accessories used:

- Connecting cables: power cable for DAD-control unit, DAD-to-front-antenna, front- to-back-antenna and wheel cable
- DAD-control unit.(For receiving the data from antenna)
- Distance-measuring wheel.
- Fully charged 12V batteries
- IDS 100 MHz Shielded antennas and connecting cable.
- IDS, 25 MHz & 40 MHz Unshielded antennas with different pole.
- Laptop carrier "backpack"
- Panasonic Toughbook (laptop) and network cable (To visualize real time GPR data acquisition)
- Pulling cables and rope for connecting the antenna boxes
- Tape (To measure the distance and indicator of Straight line).
- Toolboxes: IDS auxiliary box and the general tool box
- Trimble RTK GPS and its connecting Cable (To measure the accurate position of the location of survey starting point and ending point and elevation difference if available)

4.4.2 Data collection

The Ground Penetrating Radar used for data collection for this study is a Sensors & Software IDS S.p.A, Italy, and GRED HD. The system is equipped with a transmitter and a receiver connected with fiber optic cables to a console measuring time and reflection strength, which is connected to a Toughbook that displays a profile of the subsurface on site. There are a number of parameters that have to be set up before data collection starts. These are survey type, wheel type, terrain type, data collection mode, frequency, step size, antenna separation, time window, time sampling interval. In this present study survey data collection method is the common offset in which the transmitter and the receiver antennae are separated by a fixed distance and moved along the survey line.

4.4.3 Data processing

Data acquisition

Recording GPR-data using K2FastWave, it's a very user friendly data acquisition software. During a measurement, the GPR-signal will be shown in real time in the measurement window and you can also mark the anomaly in radar profile. In this study we follow the parameter according to antenna frequency.

Table 6 GPR setting for data acquisition

GPR parameters	Setting
GPR Antenna Frequencies	100
Range	256 ns
Maximum Antenna Separation	1 Meter
Sequence	2.2
No of Samples/Scan	512
Wheel factor	1
Ground Type	Rough or Smooth

Figure 22 GPR Data acquisition using 100 MHz

Figure 21 GPR Data acquisition using 40 MHz

Post Processing

Understanding of subsurface is necessary for processing and analysis of GPR profiles. The energy propagated in the ground by a transmitting antenna interacts with subsurface materials in many ways like attenuation, reflection, refraction and diffraction.

The raw data may not show the true subsurface image because of external noise produced by surrounding area. To reduce the noises care should be taken during data collection.

The radar profiles collected in the field were processed with GRED HD software manufactured by IDS S.p.A, Italy, the profiles were processes in the sequence starting from move profile start tome, background noise removal different filters, auto gain and migration.

4.4.4 Data Interpretation

The interpretation of GPR data is based on the characterization of specific signal patterns received from the subsurface discontinuities. To interpret GPR profiles one must be aware of field condition and survey strategies. The raw GPR data at times does not represents the real images of subsurface because of diffraction of radar energy from complex buried structure. These appear in GPR profile as a random or multiple reflection and such profiles requires special processing steps (Annan, 2003,). Previous studies suggest that for interpretation of GPR data and for locating near subsurface displacement follow some specific pattern in radargram. Identification keys of subsurface (fracture/fault) structures in radar profile are (1) a change from one radar facies to another, (2) the occurrence of gently to deeply inclined arrays of terminated reflectors which appear as a line in the radar signals, (3) a change in the frequency and/ or amplitude (Energy Loss/trace) of the radar signal, (4) a group of reflectors that end abruptly along a line, and A strong diffraction hyperbola.

4.5 ScanSAR Interferometry

In this present study have been attempted to extraction of wide-ranging crustal movement by using PALSAR ScanSAR-ScanSAR differential interferometric processing in the Himalayan frontal thrust area by using ALOS PALSAR level 0 data.

Table 7 Summary of ScanSAR RAW data.

Date_ID (Area Uttarakhand) YYYYMMDD_ID	Path	Frame no	Orbit Direction	Polarization
20080323_010	172	3000	Descending	HH5scan
20080508_009				
20081108_008				
20090208_006				
20091227_005				
20100329_003				
20100514_002				
Total Scene = 07				
Total scene (Interferometric pair) = 21				

Date_ID (Area Himachal Pradesh) YYYYMMDD_ID	Path	Frame no	Orbit Direction	Polarization
20061224_012	175	2950	Descending	HH5scan
20071227_011				
20081229_007				
20100101_004				
20110104_001				
Total Scene = 5				
Total scene (Interferometric pair) = 05				

4.5.1 ScanSAR Image Processing

(Adapted from Miyawaki, 2011 and Gamma Software)

The ScanSAR data processing for SLC generation used a "Range Doppler Algorithm" in this process to convert raw beam to SLC using each and Separate beam process

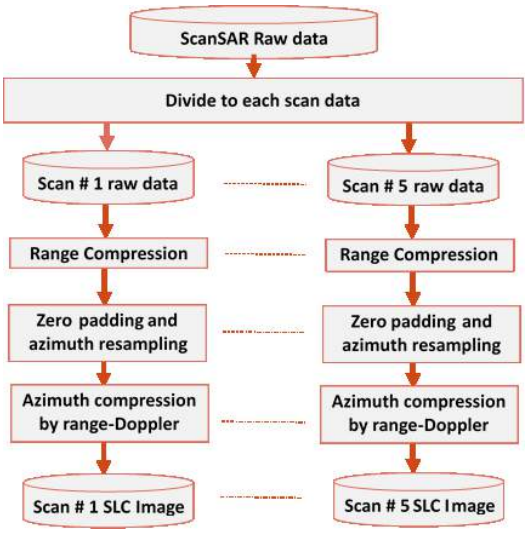

Figure 23 ScanSAR image processing flow chart (Miyawaki, 2011)

After processing of raw data we found only 9 pairs are burst sync overlap and suitable for interferometric processing. Then further processing was done on only 9 data pair.

Date_ID (Area UK), YYYYMMDD_ID		
Master	Slave	Temporal Baseline
20091227_005	20100329_003	92
20080508_009	20081108_008	184
20080323_010	20090208_006	322
20090208_006	20100514_002	460
20080323_010	20100514_002	782
Total pre-processed SLC (Interferometric pair) = 05		
Date_ID (Area HP), YYYYMMDD_ID		
Master	Slave	Temporal Baseline
20061224_012	20071227_011	368
20100101_004	20110104_001	368
20071227_011	20100101_004	736
20061224_012	20100101_004	1104
Total pre-processed SLC (Interferometric pair) = 04		

ScanSAR-ScanSAR differential interferometric processing

Methodology for ScanSAR interferometry

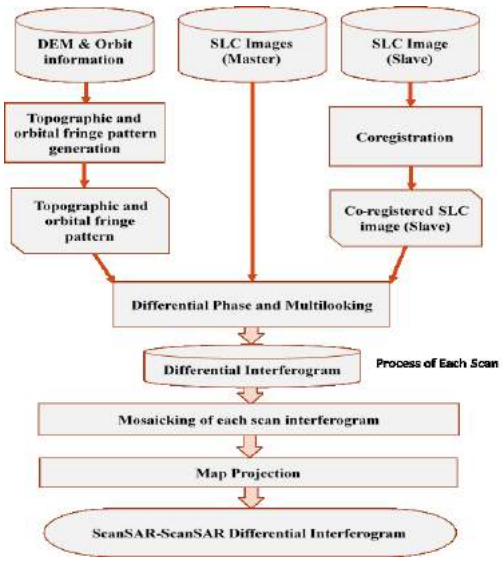

Figure 24 ScanSAR-ScanSAR differential interferometry flow chart (Miyawaki, 2011)

The ScanSAR-ScanSAR differential interferometric processing with master and slave SLC image is calculated at each scan. The processing overview is as follows:

- Coregistration of slave SLC image to master image.
- Topographic and orbital fringe pattern generation using DEM and orbit information.
- Generation of differential interferogram by phase difference of co-registered master - slave SLC images, and topographic and orbital fringe pattern.
- Multi-look processing.
- Mosaicing of differential interferograms of each scan.
- Map projection.

The overall methodology using GAMMA software using command line.

5 RESULTS AND DISCUSSION

This chapter provides a discussion of the results obtained by using Terrain profiling, Drainage analysis, GPR data acquisition and SAR data analysis. The answers of the research questions will be given in light of the results and discussed in order to meet the objectives of the research.

5.1 Geomorphological Analysis

The anomalies we identified consist of river diversions, shifts in channel pattern and longitudinal changes of the channel behavior. Due to their size, they are suggestive of the presence of active tectonic structures. A number of broad scale drainage anomalies have been identified in the area. Drainage properties can be well diagnosed by image interpretation method. Detailed categorization of drainage pattern can attribute each pattern to specified terrain settings. However, there can also be many distortions in expected drainage pattern. These distortions, the so-called drainage anomalies, are widely observed in the study area.

The morphological analysis carried out in this work revealed the occurrence of several anomalies of the drainage network in the Himalayan front thrust consisting mainly in river anomaly. Changes in the channel pattern were highlighted in the HFT especially in which five basin were studied in better detail. The analysis of all noticeable drainage systems and their patterns in the HFT provides a detailed understanding about the type of drainage distortion at all sites in the area.

5.1.1 Topographic analysis

Transverse and Longitudinal topographic profiles across the piedmont plain (five basin) extracted from the Cartosat-1(10 m) DEM.

Dhela basin Ramnagar, UK

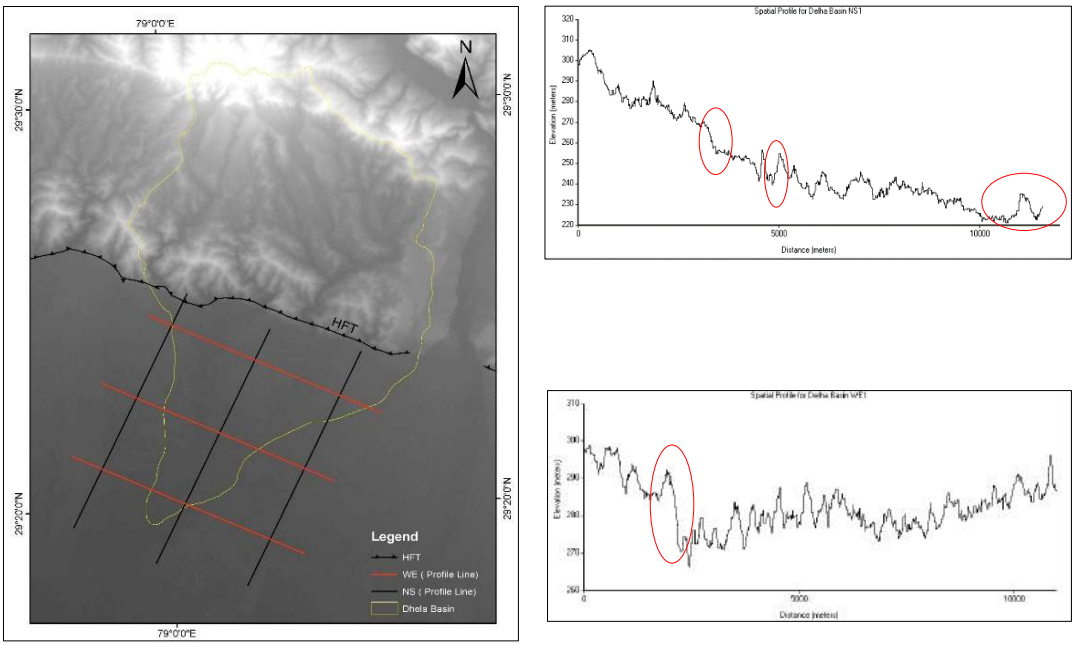

Figure 25 Terrain profile of Dhela Basin, Ramnagar, UK

Khoh Basin, Kotedwar, UK

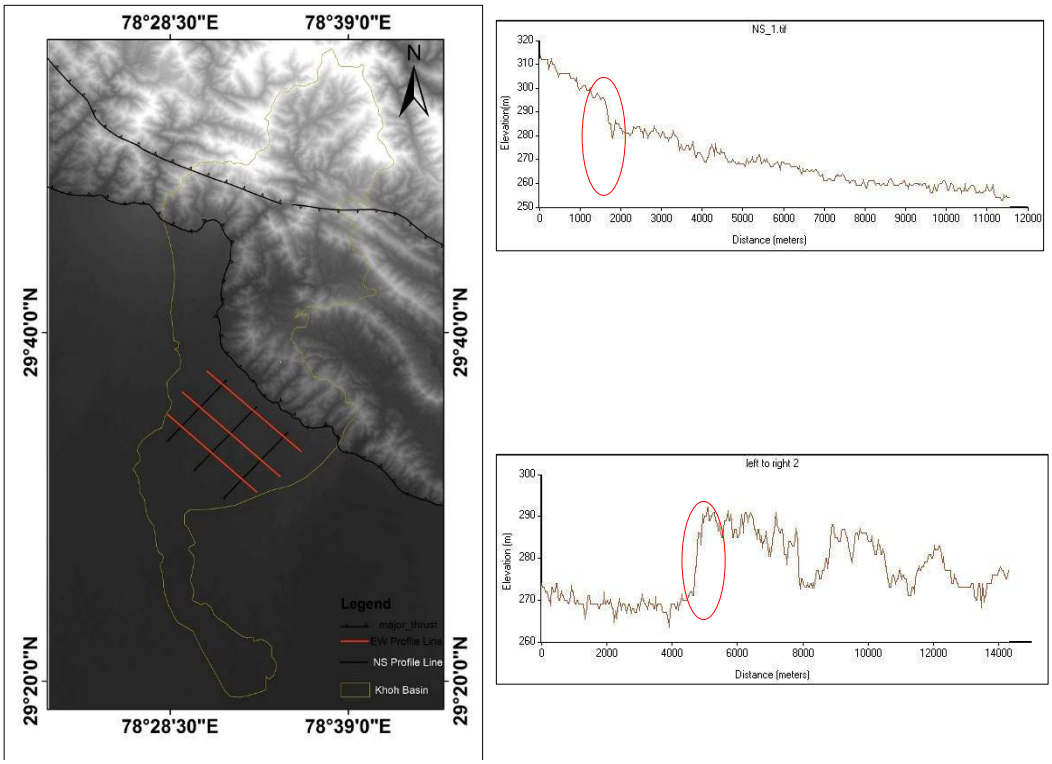

Figure 26 Terrain profile of Khoh Basin, Kotedwar, UK

Solani Basin, Mohand area, UK

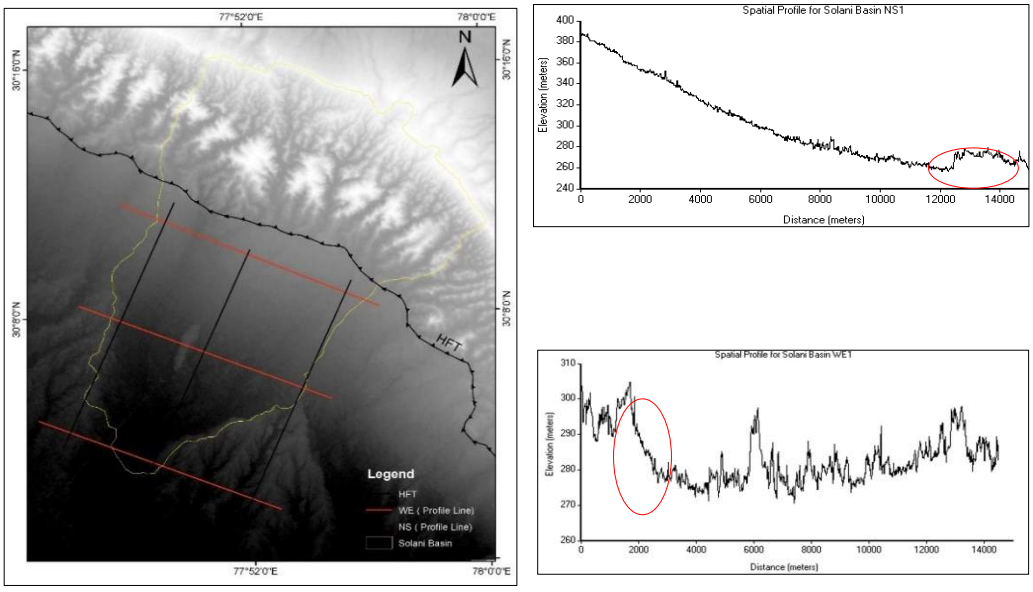

Figure 27 Terrain profile of Solani Basin, Mohand area, UK

Markanda Basin, Kala-Amb (Part of UK, HP and Haryana)

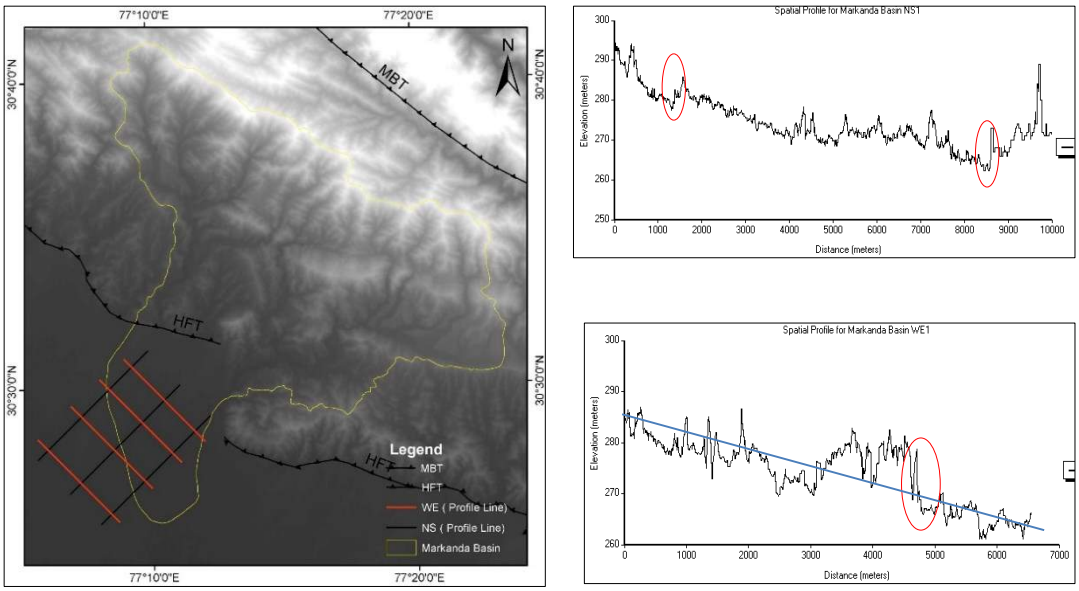

Figure 28 Terrain profile of Markanda Basin, Kala-Amb (Part of UK, HP and Haryana)

Rupnagar Basin, Part of Chandigarh & Punjab

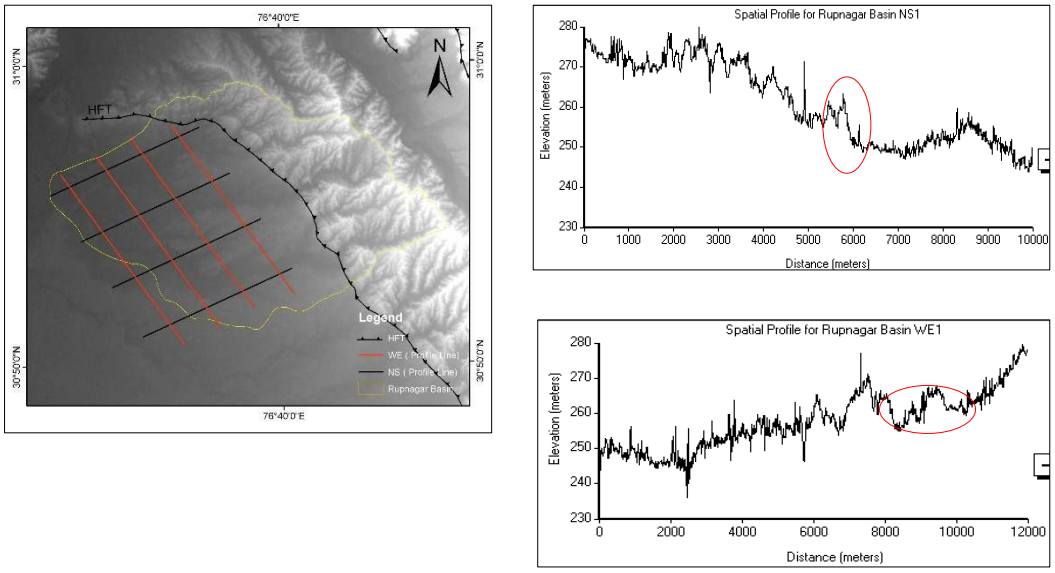

Figure 29 Terrain profile of Rupnagar Basin, Part of Chandigarh & Punjab

All terrain profiles are taken in piedmont area in Dhela, Khoh, Solani, Markanada and Rupnagar basin, in transverse and longitudinal direction in order to understand and quantify the marked differences in elevation within the basin.

The geomorphology of alluvial fan is affected by climate and geology of the area, the geomorphic evolution of alluvial fans is controlled by catchment characteristics (including drainage basin area, relief and geology), tectonics and climate (Harvey et al 2005). The Himalayan Piedmont Zone has formed as a result of coalescing alluvial fans, alluvial aprons and talus deposits. The fans have differential morphologies and aggradation processes within a common climatic zone and similar litho-tectonic setting of the catchment area.

The transverse and longitudinal show complex shape in piedmont area. Normal dipping of terrain profile indicate drainage valley and the abrupt change in terrain profile indicate surface upliftment or active buried structure in piedmont zone. Sudden change in topographic profile in alluvial plain may indicate fault scarp. In terrain profiling mark the area where sudden elevation break in order of 5 meter or more than 5 meter.

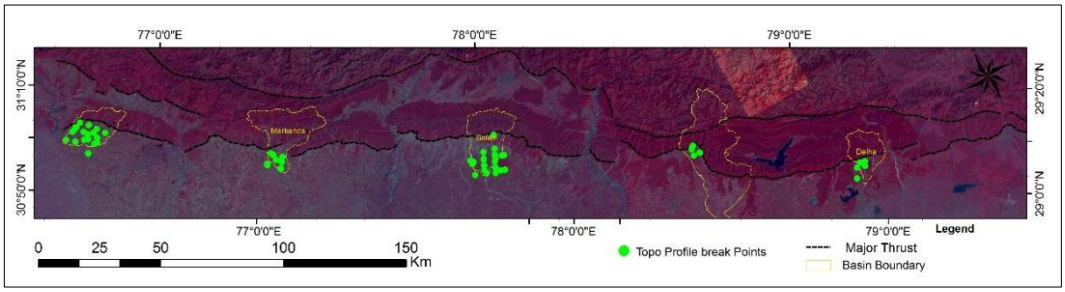

Figure 30 Overall Terrain Break point map

In the above figure green dot are showing abrupt topographic break point. All break points are identified in respective basins.

5.1.2 Lineament Mapping

"A lineament is defined as large scale linear feature, which expresses itself in terms of topography of the underlying structural features."

Lineament describe the hidden architecture of subsurface in terms of long linear pattern in aerial and satellite imageries. Lineaments mapped by surface indicator as linear ridge or valley, Straight line River orientation, abrupt change of river along the line, sudden break of elevation jointed as a long line, Linear vegetation pattern, the describe surface indictors are may be fault line, fracture and Dykes. According to National geomorphological lineament mapping (NGLM) Lineament size should be minimum 300 meter. In satellite imagery the lineament is clearly visible as a linear or curvilinear feature .The some key feature on the earth surface the lineament is identified by

1. Abrupt topographic break.
2. Lithology change
3. Rectilinear stream or follow the single line
4. Surface depression or valley in a liner or curvilinear,
5. Vegetation arrangement is looks as line
6. Vegetation height changing and type of vegetation,

The mapping of lineament is based on satellite imageries or aerial photograph to follow the basic preprocessing on satellite data for removal of extra tonal variation or noise in the imagery. Processed data should be mosaicked a large data sets then can identify and map the large scale lineament pattern as well as regional setting of lineament in the area. Microwave ScanSAR data is more use full to map lineament and structural feature. In this present study the lineament identified from the different data as ScanSAR Microwave data, Multispectral data or previous literature mapped lineament, show that a few of them trend parallel to the Himalayan orogeny, and the others are transverse to it. The lineament rose diagram clearly indicate the effect of the tectonic activity in the study area. The lineament also helpful to integrated study to identifying the probable GPR sites.

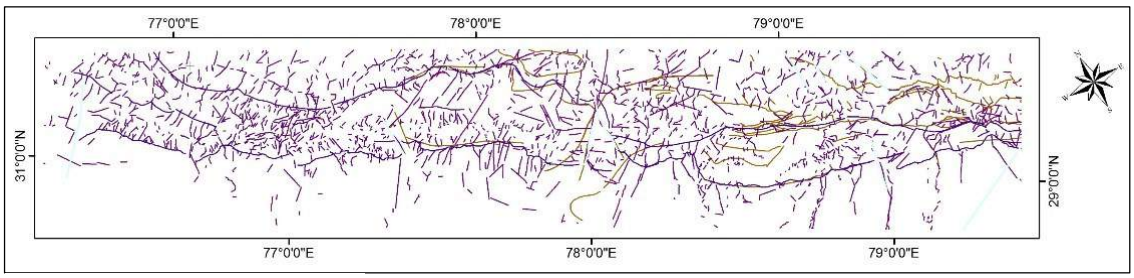

Figure 31 Lineament Map

The overall mapped lineament direction showing NE-SW direction and its matched with Himalayan orogeny trend.

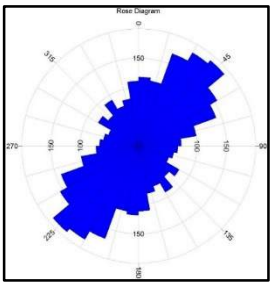

Figure 32 Rose diagram of lineament

5.1.3 Drainage Anomaly

In this study, several steps for drainage pattern analysis were used to reveal different drainage anomalies. The analysis of satellite images as a first step was followed by comparison with the Howard catalogue of drainage patterns (Howard, 1967). Recognition of abnormalities in drainage patterns was conducted and the mechanism behind their distortion was interpreted.

Brief explanation of the drainage anomalies, which we mapped in our study area.

Table 8 Brief explanation of drainage anomaly

Drainage anomaly	Description	Reason for anomaly
Rectilinearity of Streams	Long rectilinear segment of stream when the regional drainage pattern is other than rectangular.	It indicates that the stream is flowing along a fault, fracture or easily erosible vein or dyke
Abrupt and localised meanders in streams	Its represents interruption in normal pattern related to subtle upstream reduction in stream gradient.	Its indicate the occurrence of a dome-like feature along the course of the stream which may be an active zone of uplift
Compressed meanders	Several meanders of stream are squeezed, compressed and incised.	Its indicate the occurrence of fault, fold or Domal structure across the course of the stream or a plunging fold with plunge towards upstream
Abrupt and localised braiding	Local acquisition of coarser bed load. Loss of flow volume due to local increase in channel-bed infiltration and under flow. Loss in flow velocity due to local increase in flattening of gradient	Indicate the appearance of rocks types with sharp difference in hardness and infiltration capacity and/or the occurrence of local structure.
Anomalous pinching or flattening of streams	Local Narrowing and widening of channels.	It indicate the occurrence of local structure or appearance of rock types with sharp difference in hardness.
Anomalous curves or turns of the streams	Presence of an isolated pond, marsh or alluvial fill along the path of mature stream	It indicates the presence of surface or near surfaces across the path of the stream viz., acute or obtuse elbow turn indicates fault, round turn around an area indicates sub-surface high.

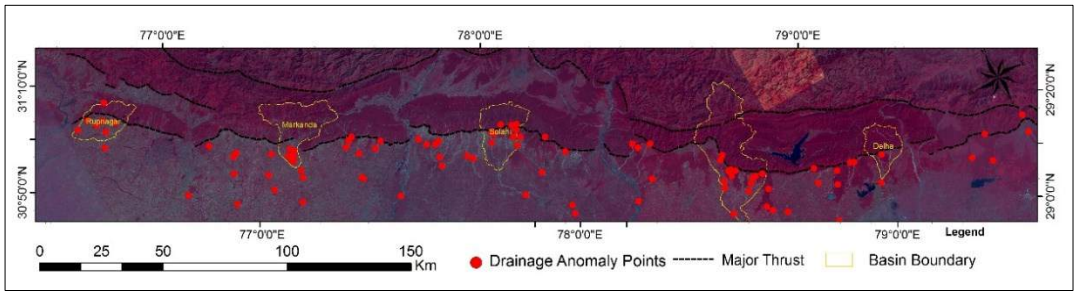

Figure 33 Overall Drainage Anomaly Point map

Figure showing drainage anomaly point over LISS III mosaicked image

5.1.4 Drainage migration/ Shift/ Capturing

Most of the available cases of river shifts in the Himalayan foothill basin are characterized by the (1) migration of a deflection point of the river along structural trends, (2) drainage, follow along the fault line, (3) generation of compressed meandering, (4) the general trend of migration of river is towards the Eastward side.

The active fault zonation involved in the process of shifting/migration of the fluvial drainage in and around four Basins (Dhela, Khoh, Solani, Markanda) were found active during the study dataset (period of approx. 41 years), and they are compatible with the present seismotectonic activity of the regions under consideration. In Rupnagar basin and surrounding we did not find any Drainage migration/ shifting may be due to anthropogenic activity.

The anomalies we identified consist in river diversions, shifts in channel pattern and longitudinal changes of the channel behavior. Due to their dimension, they are suggestive of the presence of active buried tectonic structures. Drainage migration analysis have been done by careful observation of temporal satellite imagery. Their origin was assessed by temporal remote sensing data comparison between 1980, 1998 and 2013 Landsat Images.

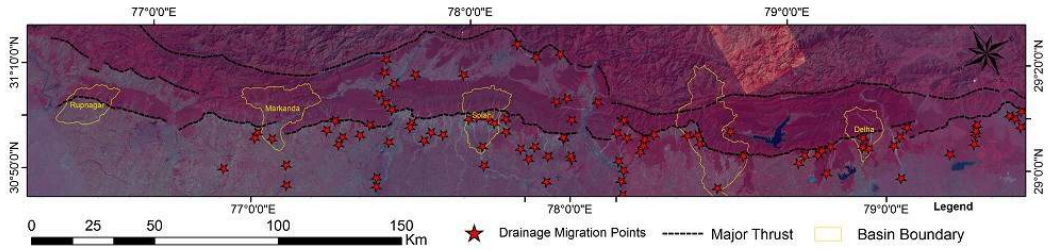

Figure 34 Overall Drainage migration Point map

In the above figure the star points indicate the drainage migration in the four basin viz., Dhela, Khoh, Solani and Markanda. Drainage shifting activity were found more in easter side of the HFT and decreases as we move towards western side of the HFT.

5.1.5 Combined map of Drainage anomaly, Drainage Migration and Topo-break profile maps in separate basin.

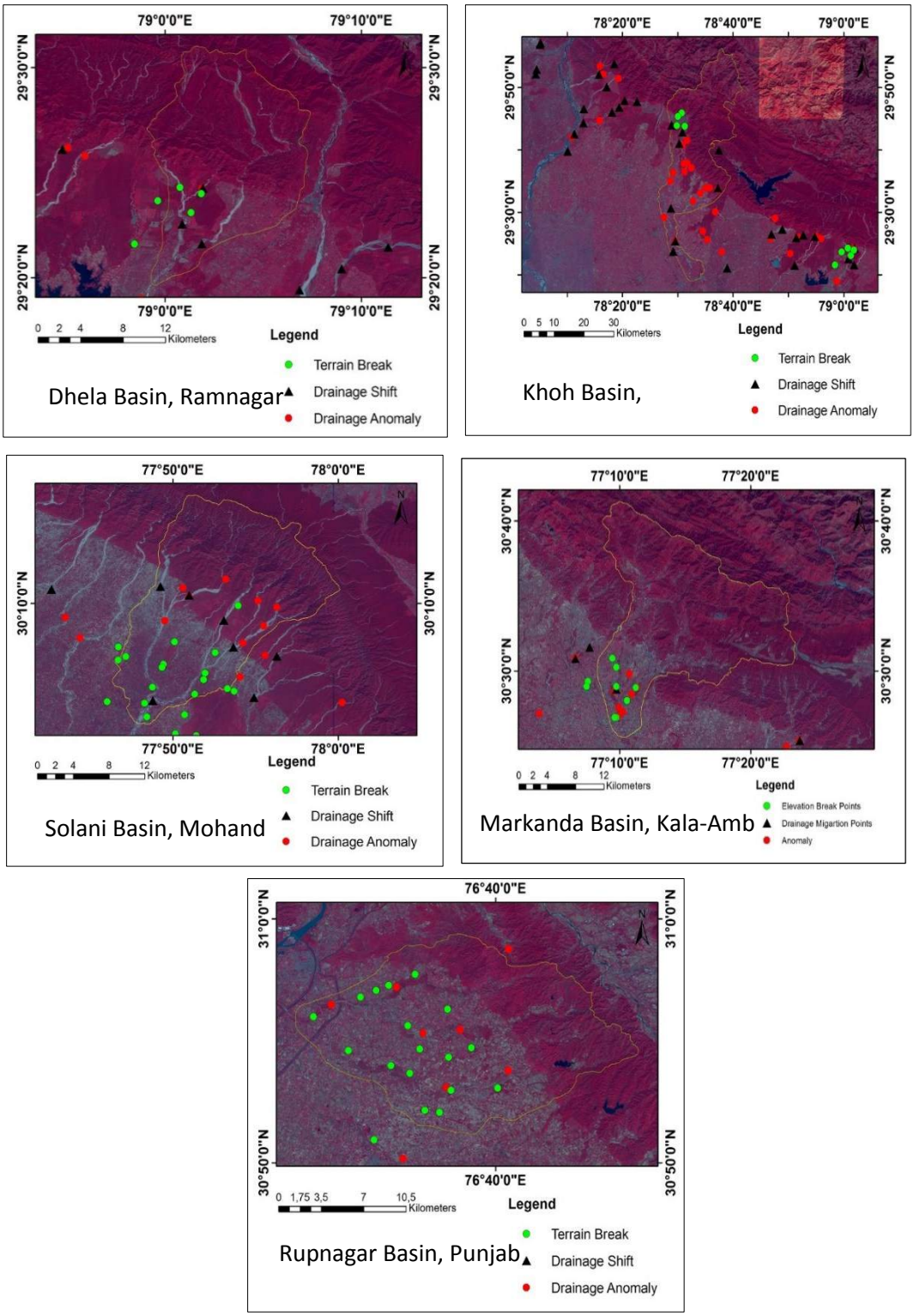

Figure 35 Individual basins showing all anomaly points

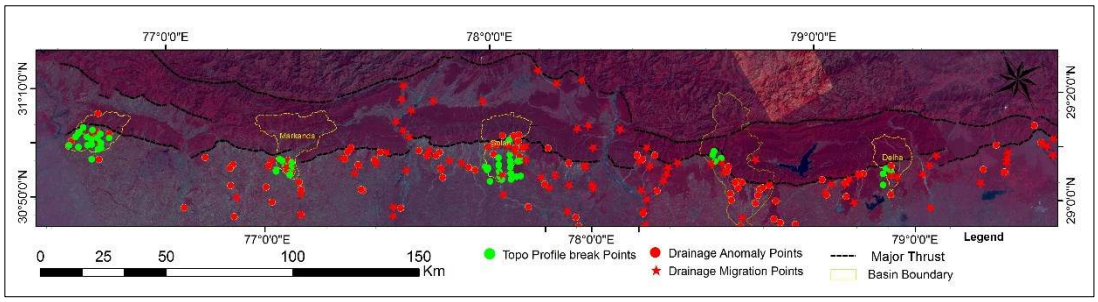

Figure 36 Study area showing all anomaly

Above figure shows the integrated occurrence of drainage anomaly, drainage shift/migration and topographic break.

By integrating the topographic break, trends of lineament, drainage anomaly and drainage migration/shift, observation were made to correlate, to account for the probabilistic fault activity of the region. The regions where the co-occurrence of lineament, topographic break, drainage anomaly and drainage migration/shift chances , the area were scrutinized using GPR survey for verification of probable active faults.

5.2 Ground Penetrating Radar

Ground-penetrating radar (GPR) is a convenient high resolution geophysical instrument in the search and detection of subsurface fractures and fault. The main goal of this study was to evaluate the ability of GPR, using 100 MHz and 40 MHz antennae, to locate shallow active fault in several test sites over Himalayan piedmont plain. The result demonstrates that faults and fault zones produce a variety of signatures on GPR data according to antenna frequency, orientation and heterogeneity of the faulted material. In terms of antenna performance, the 100 MHz data provided a higher resolution and 10 m depth penetration but in case of 40 MHz antenna, it gives low resolution but penetration depth up to 30 m.

In order to identify and characterize fracture/fault, some radargram interpretation criteria we found useful were.

- A change from one radar facies to another.
- The occurrence of gently to deeply inclined arrays of terminated reflectors which appear as a line in the radar signals.
- A change in the frequency and/or amplitude of the radar signal.
- A group of reflectors that end abruptly along a line.
- A strong diffraction hyperbola

We attempted each of these criterion in the present study

5.2.1 GPR Survey on Himalayan Foothill area

- **Site 1**

Site 1 is located in Rupnagar basin near village Rampur-Purkhali, Punjab, India. The survey site was along Haripur Nala along the drainage deflection in NW-SE direction.

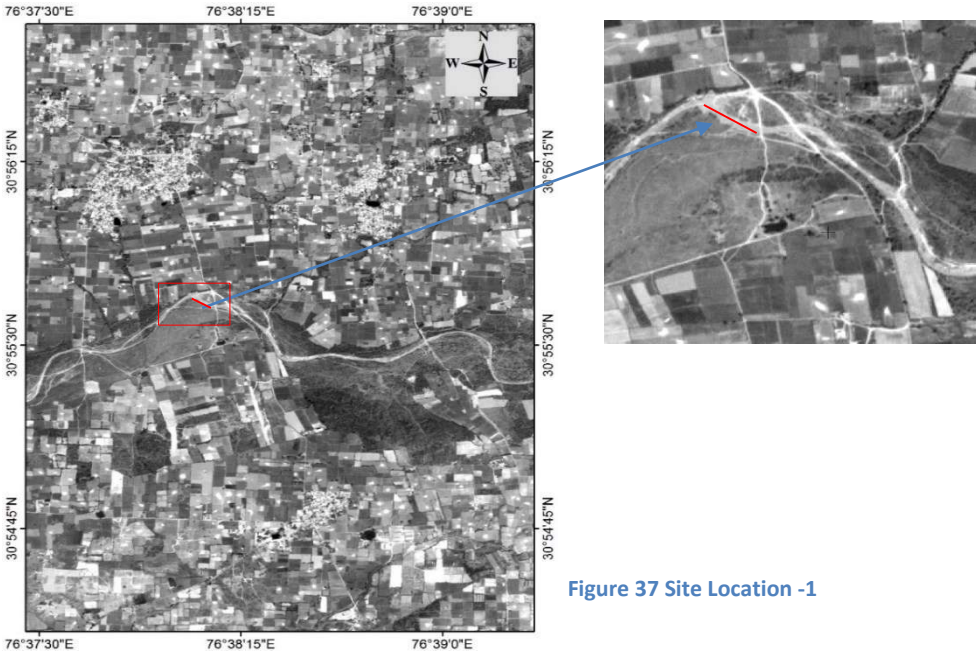

Figure 37 Site Location -1

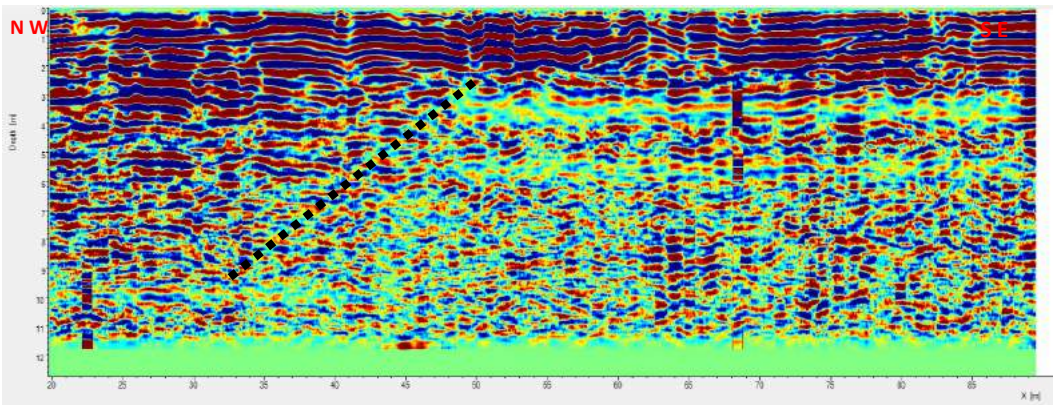

Figure 38 Processed GPR Profile site-1

Above figure shows the processed subset and interpreted data of 100 MHz GPR profile in Rupnagar basin site location-1, the 100 MHZ antenna profile shows clear reflector in upper side and, below 3 m one radar faces to another radar face. Black dotted line may be probable location of subsurface fault.

- **Site 2**

Second Site was selected near Abhipur village, Punjab, India, where survey was carried out along Budki River. This location is marked by terrain profiling and drainage anomaly. The location is marked in subset of image in green line.

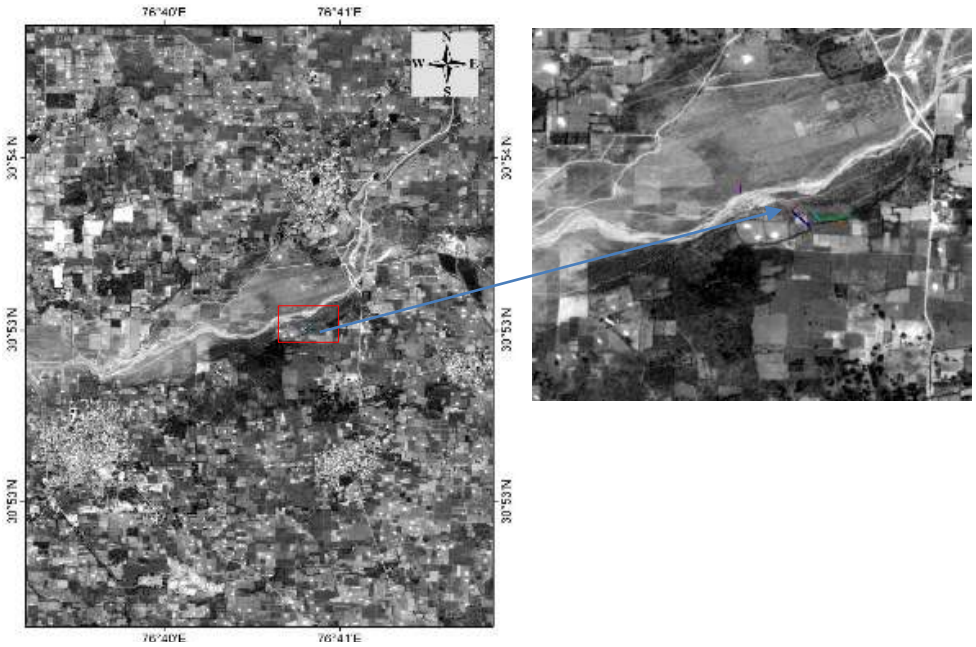

Figure 39 Site Location -2

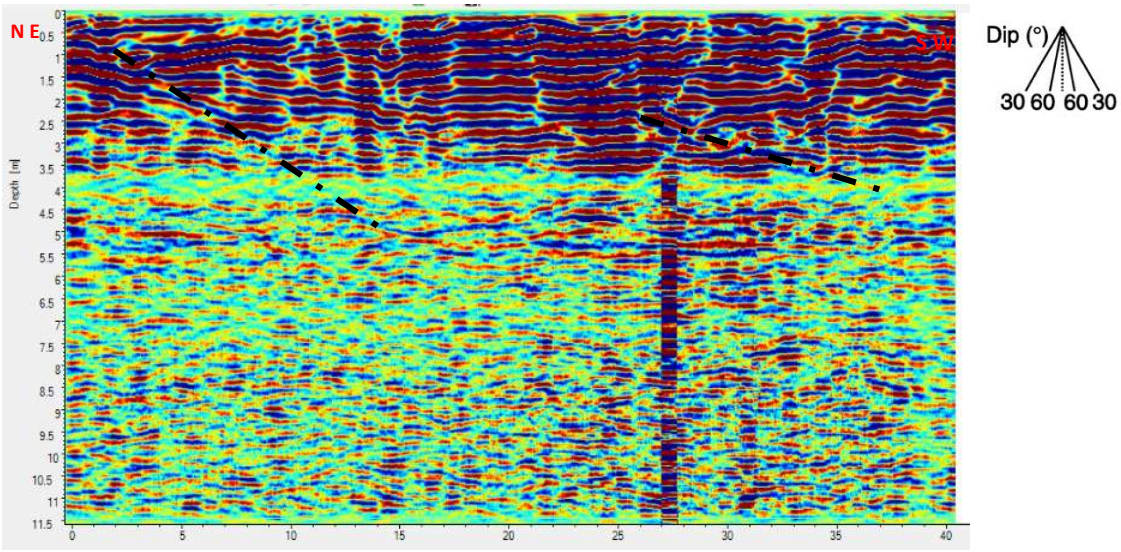

Figure 40 Processed GPR Profile site-2

The above GPR profile showing dipping direction of bed starting from 1 m depth to 4 m depth, again dipping direction is visible in moderate resolution. One another reflection found starting from 26 m. dipping feature about 40^0 SW at upper left is likely a fault.

- **Site 3**

The survey site 3 is located in the northern part of Chandigarh town near Mansa Devi Temple in the campus of soil water conservation department Chandigarh. GPR Profiles taken from NE - SW direction for location A.

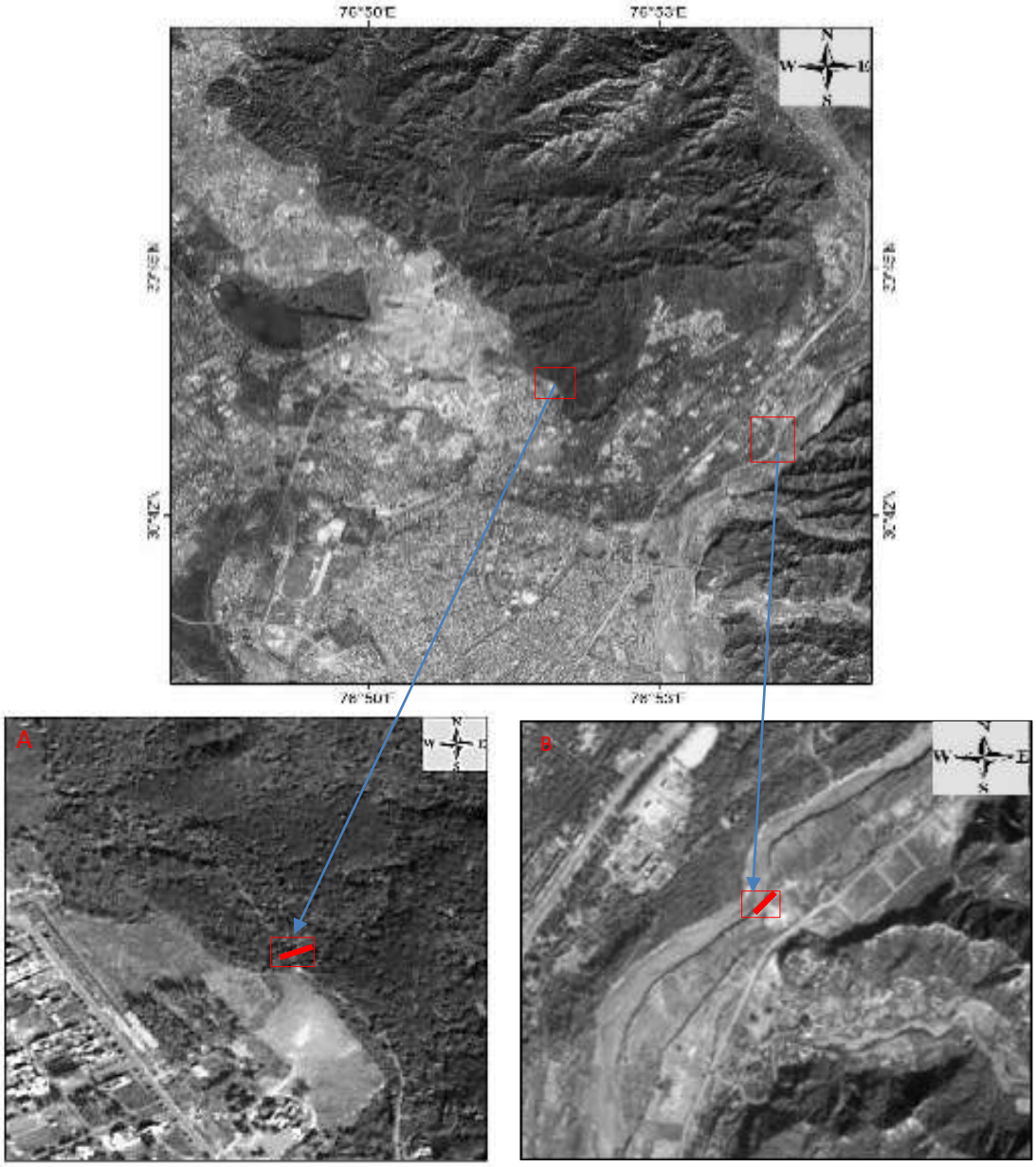

Figure 41 Site Location-3

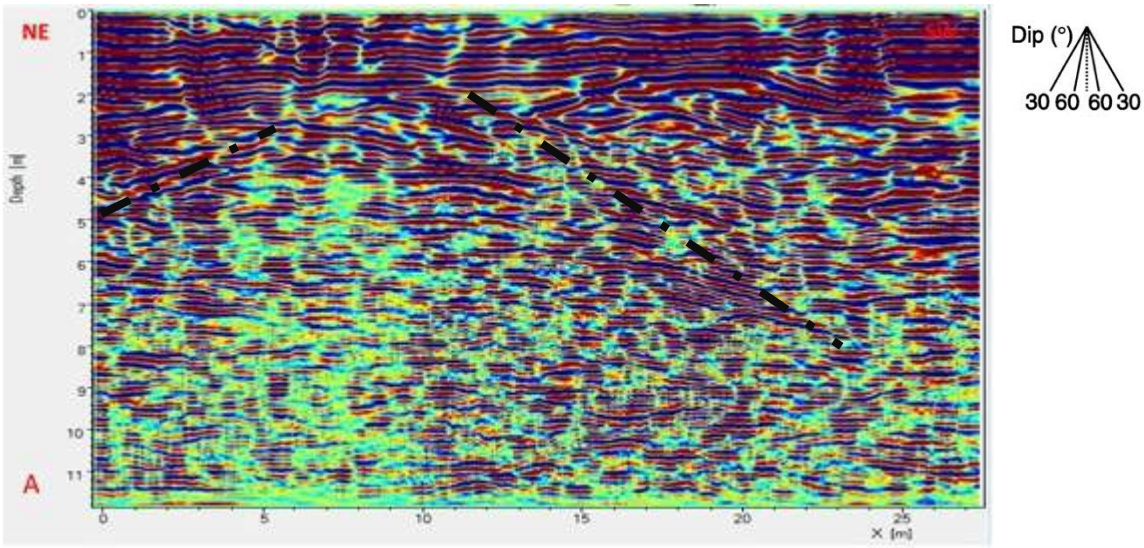

Figure 42 Processed GPR Profile Site – 3A

Figure show the processed and interpreted data of the 100 MHz GPR in chandigarh site profile taken in direction of NE to SW direction. Radargram showing different dipping direction, from 1 to 5 meter its showing northwesterly direction (20^0-35^0NE) after 5 m southwesterly dipping reflection with limited lateral continuity, reflection have moderate (30^0-40^0 SW) dips. In 15 meter in some dipping beds have terminated, right side reflector are horizontal. Blacked dotted line may be a fault line.

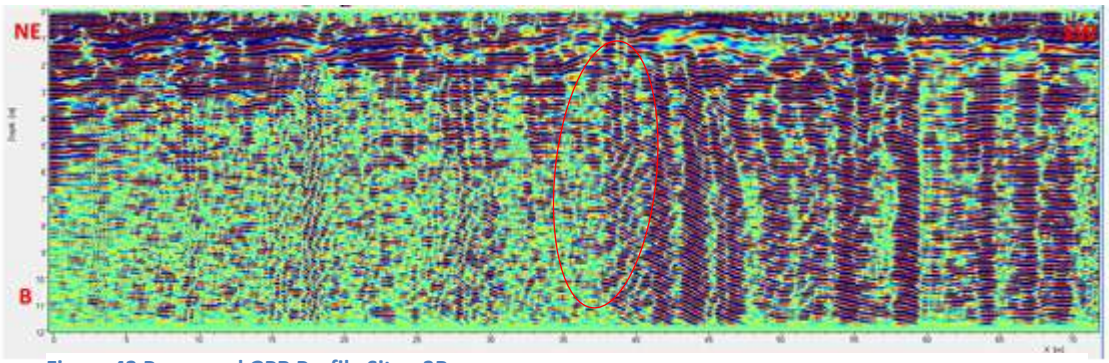

Figure 43 Processed GPR Profile Site - 3B

Above figure shows the processed GPR profile taken with the 100 MHz antenna along the Ghhagar river in direction from NE to SW. disturbance of GPR reflectors between 35 to 40 m along the profile are interpreted as deformation zone .

- **Site 4:--** GPR profile was taken along Thathar ki Nadi near Govindpur Village in Haryana which was near to HFT.

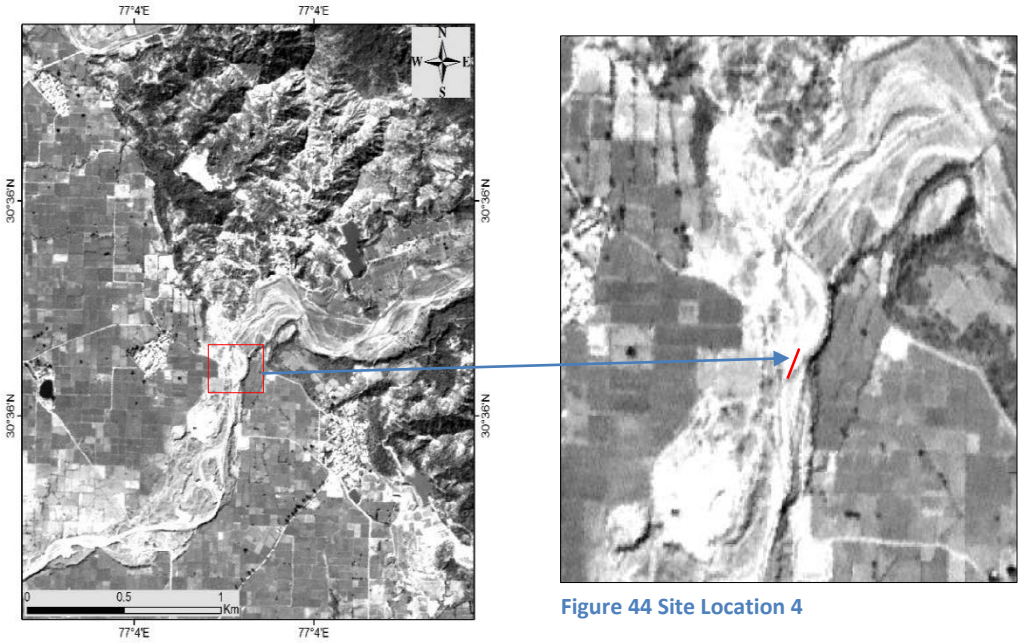

Figure 44 Site Location 4

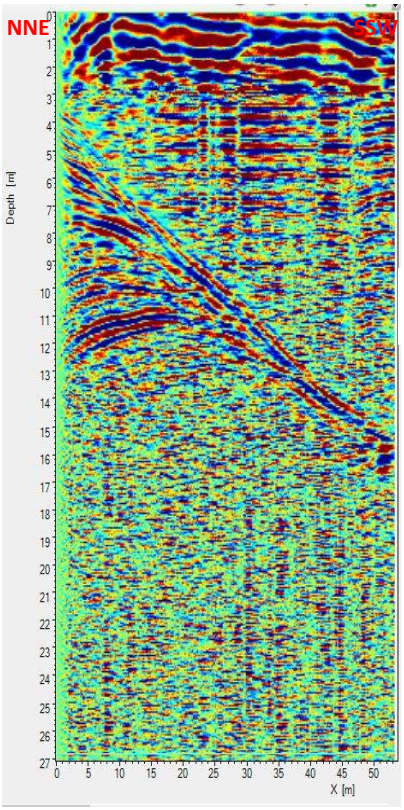

Figure 45 Processed GPR Profile in NNE-SSW direction across fault line.

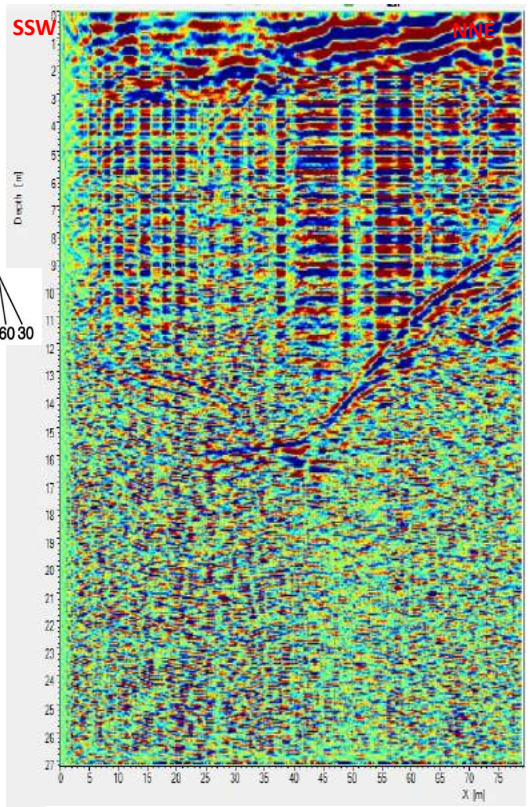

Figure 46 Processed GPR Profile across fault line in reverse direction (SSW-NNE)

In the above figure showing the result of site 4, processed GPR 40MHz antenna across the fault line in direction NNE to SSW. A clear reflectors approx. (30^0 SSW) along GPR Profile line

in depth of 5m to 16 m. a reverse profile was taken on same direction verified the GPR reflectors.

- **Site 5**

Survey was carried out in the Kutubpur, near Bhauwala Dehradun, India in direction of NNE to SSW.

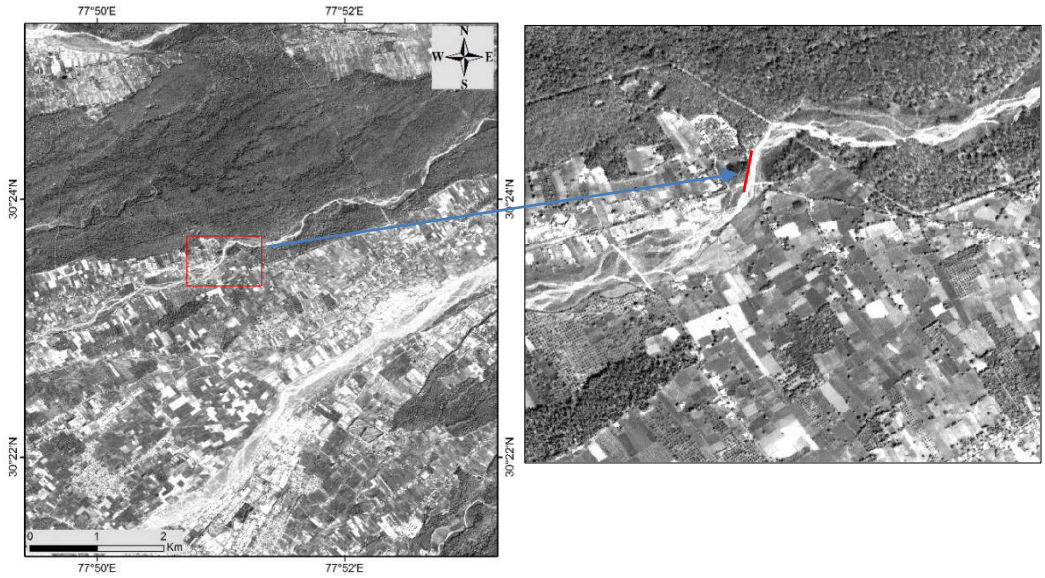

Figure 47 Site Location -5

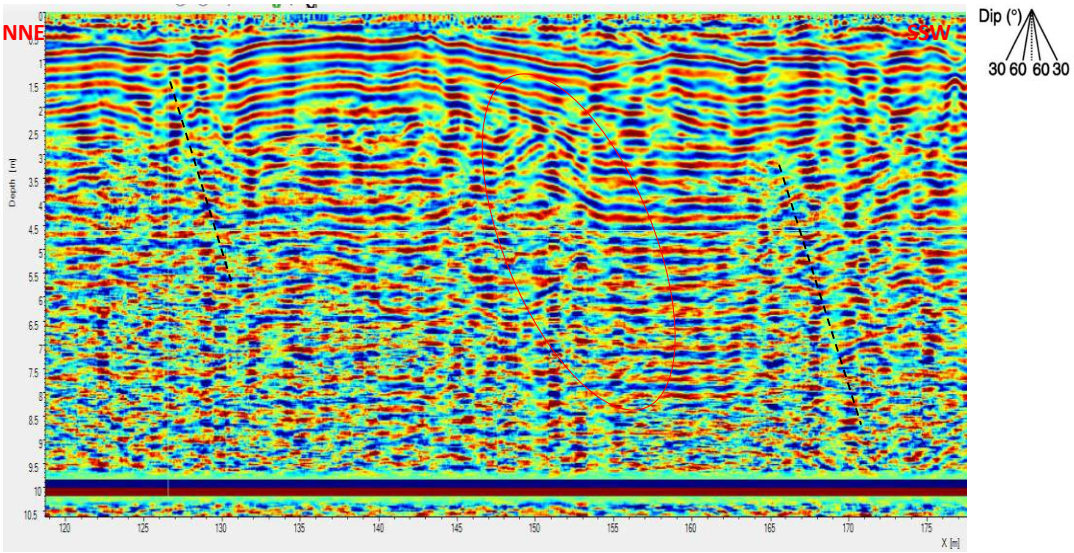

Figure 48 Processed GPR profile

Figure showing subset of radar profile GPR profile acquired using 100MHz antenna. Dipping radar reflector showed abrupt change in right side of profile and in the middle, and some disturbance in radar reflector along the left side.

5.3 ScanSAR-ScanSAR Interferometry

The processing of 12 individual Scan-SAR data has been successfully completed from raw level (ALOS PALSAR -L0) data to SLC and ground range form, covering Indo-gangetic plain to MCT. Co-registration of 12 pairs of individual beam is a pre-requisite for the generation of differential interferograms. Out of 12 Scan-SAR dataset, 7 data belongs to Uttarakhand region (with a possible 21 pair combination) where the remaining 5 data belong to Himachal Pradesh (with a possible 10 pair combination). Of the total 31 possible interferogram pair, only 9 pair satisfied the burst sync criterion. The 9 pairs were fully processed and D-InSAR images were generated.

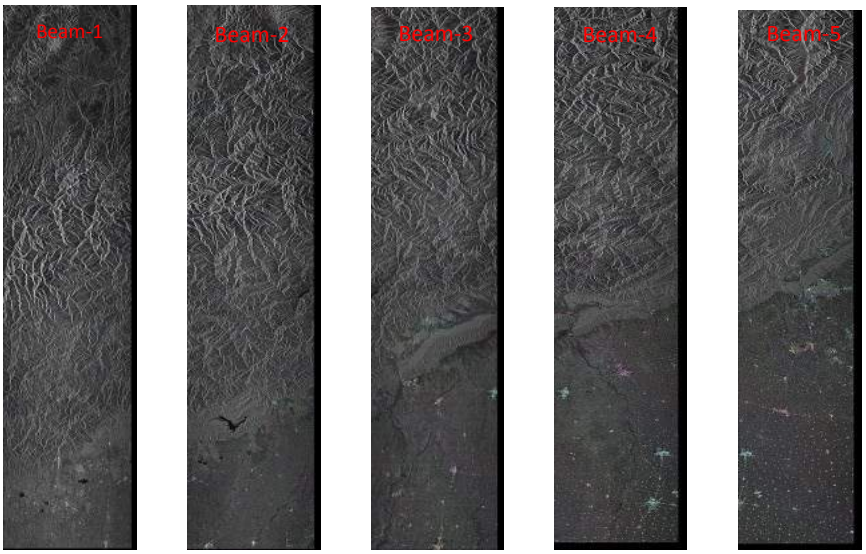

Figure 49 Differential Interferometry of each beam

Figure 51 Multi-beam D-InSAR mosaic of UK PALSAR pair

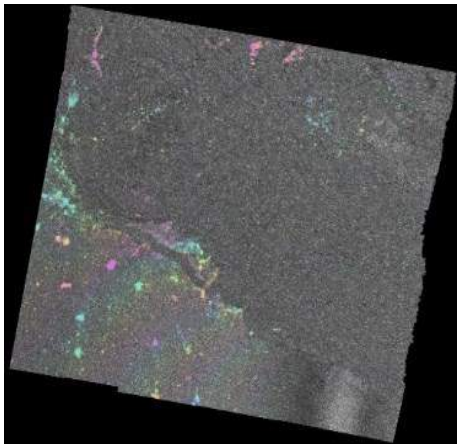

Figure 50 Geocoded Filter D-InSAR images

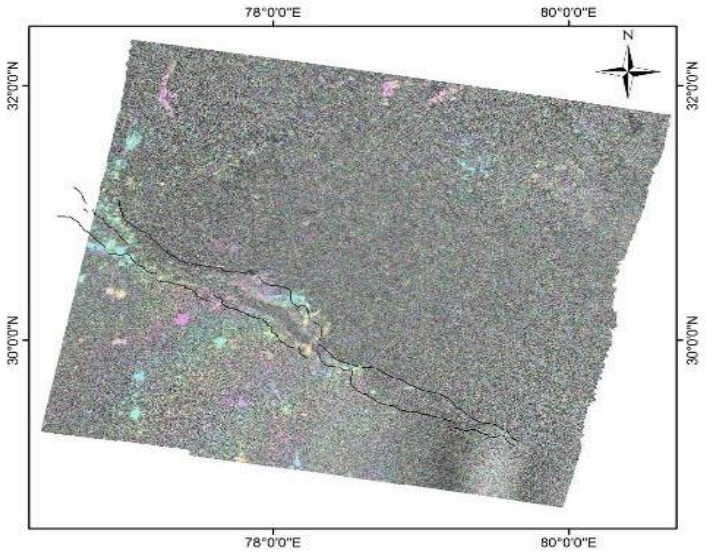

Figure 52 Geocoded filter ScanSAR-ScanSAR Images with Major thrust

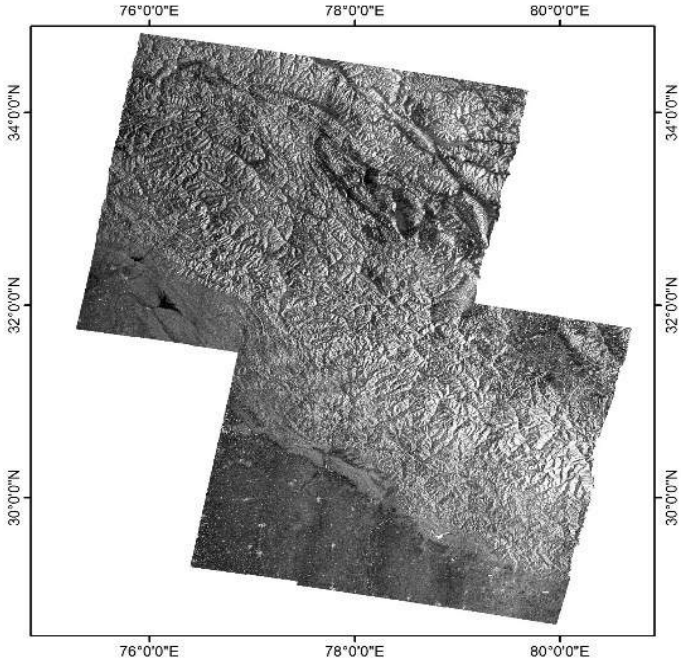

Figure 53 Mosaicked ScanSAR MLI image

The multi-look ground range image of Scan-SAR is very useful for regional mapping of structural features in the Himalayan region.

6 CONCLUSIONS

The present study has attempted to identify tectonically active zone, possible locations of active faults their relation between surface indicators like drainage anomaly, trends drainage shift and subtle topographic breaks. The integrated approach comprising multi temporal satellite data analysis, high resolution topographic analysis, drainage anomaly analysis supported by field check and GPR survey have made it possible to identify the probable locations of active faults in the study area by using geophysical signature like termination of radar reflectors, dipping layers of reflection along the fault line and changes in facies of reflectors, corroborate the location of a fault with subsurface evidence.

The following conclusion were drawn.

- Drainage anomaly and topographic anomaly analysis using multi-temporal satellite images and high resolution DEM could efficiently identify the probable locations of active fault.
- GPR survey successfully confirmed the presence of active faults based on the geometry of the subsurface layers upto a depth of ~ 30m.
- DInSAR analysis using ScanSAR data could provide preliminary deformation phase pattern in the differential interferogram which require further analysis and additional data for the preparation of horizontal strain accumulation and displacement scenario.

6.1 Recommendations

There are few things which can be taken further to carry out this work further to different direction. They are mentioned as below. Recommendations for the future work are as follows:

- The GPR survey technique should be applied in 3-D mode for better characterization of subsurface fault. Further study should be conducted in another location where high active zone was found in present study area.
- For better assessment of ScanSAR Differential interferometry more datasets should be used and high resolution DEM used for topographic noise removal.
- Detail Geological map (1:25000) of the area can be beneficial in respect of Georadar reflector characteristics in terms of lithology.

REFERENCES

Annan, A.P. 2009. “Chapter 1 – Electromagnetic Principles of Ground Penetrating Radar.” In *Ground Penetrating Radar*, Chapter 1:1–40.

Arthur David Howard. 1967. “Drainage Analysis in Geologic Interpretation: A Summation.” *AAPG Bulletin* 51 (11).

Berryman, K., Ries, W. & Litchfield, N., 2014. *The Himalayan Frontal Thrust : Attributes for seismic hazard*, Global Eathqauke Model.

Bettinelli, Pierre, Jean Philippe Avouac, Mireille Flouzat, François Jouanne, Laurent Bollinger, Pascal Willis, and Gyani Raja Chitrakar. 2006. “Plate Motion of India and Interseismic Strain in the Nepal Himalaya from GPS and DORIS Measurements.” *Journal of Geodesy* 80 (8-11): 567–89.

Bhatt, C. M., P. K. Litoria, and P. K. Sharma. 2008. “Geomorphic Signatures of Active Tectonics in Bist Doab Interfluvial Tract of Punjab, NW India.” *Journal of the Indian Society of Remote Sensing* 36 (4): 361–73.

Bilham, Roger, Kristine Larson, and Jeffrey Freymueller. 1997. “GPS Measurements of Present-Day Convergence across the Nepal Himalaya.” *Nature* 386 (6620): 61–64.

Bubeck, A., M. Wilkinson, G. P. Roberts, P. a. Cowie, K. J W McCaffrey, R. Phillips, and P. Sammonds. 2014. “The Tectonic Geomorphology of Bedrock Scarps on Active Normal Faults in the Italian Apennines Mapped Using Combined Ground Penetrating Radar and Terrestrial Laser Scanning.” *Geomorphology*.

Burrato, Pierfrancesco, Francesca Ciucci, and Gianluca Valensise. 2003. “An Inventory of River Anomalies in the Po Plain, Northern Italy: Evidence for Active Blind Thrust Faulting.” *Annals of Geophysics* 46 (5): 865–82.

Caijun, X., Hao, W. & Guoyan, J., 2011. Study on crustal deformation of Wenchuan Ms8 . 0 earthquake using wide-swath ScanSAR and MODIS. Geodesy and Geodynamics, 2(2), pp.1–6.

Cluff, L. S., C. R. Allen, and J. L. Sherard. 1974. “Potentially Active Faults in Dam Foundations.” *Géotechnique*.

Copley, A. et al., 2014. Active faulting in apparently stable peninsular India : Rift inversion and a Holocene-age great earthquake on the Tapti Fault. Journal of Geophysical Research, pp.1–17.

Cui, Xi’ai, Qiming Zeng, Cunren Liang, and Jian Jiao. 2010a. “Investigating Co-Seismic Deformation of the 2008 Wenchuan Earthquake with ALOS SCANSAR Interferometric Observations.” *International Geoscience and Remote Sensing Symposium (IGARSS)*, 4612–15.

Curry, Adam. n.d. “Using GPR to Understand Active Faults: A Case Study from the Whakatane Graben, New Zealand.”

Demanet, D. et al., 2001. Application and processing of geophysical images for mapping faults. *Computers and Geosciences*, 27(9), pp.1031–1037.

Federico, C, and Universita Geologia. 2014. “2D-3D GPR as an Efficient Tool for Paleoseismology : A Successful Case History across the Castrovillari Fault (Southern Apennines , Italy).” *15 Th International Conferences on Ground Penetrating Radar - GPR 2014*, 947–52.

Ferry, Matthieu, Mustapha Meghraoui, Jean François Girard, Thomas K. Rockwell, Özgur Kozaci, Serdar Akyuz, and Aykut Barka. 2004. “Ground-Penetrating Radar Investigations along the North Anatolian Fault near Izmit, Turkey: Constraints on the Right-Lateral Movement and Slip History.” *Geology* 32 (1): 85–88.

Green, A. et al., 2003. Results of 3-D georadar surveying and trenching the San Andreas fault near its northern landward limit. *Tectonophysics*, 368(1-4), pp.723.

Gross, R. et al., 2004. Location and geometry of the Wellington Fault (New Zealand) defined by detailed three-dimensional georadar data. *Journal of Geophysical Research: Solid Earth*, 109(5), pp.1–14.

Gross, Ralf, Alan G. Green, Heinrich Horstmeyer, and John H. Begg. 2004a. “Location and Geometry of the Wellington Fault (New Zealand) Defined by Detailed Three-Dimensional Georadar Data.” *Journal of Geophysical Research: Solid Earth* 109 (5): 1–14.

Hooper, Andrew, David Bekaert, Karsten Spaans, and Mahmut Arıkan. 2012. “Recent Advances in SAR Interferometry Time Series Analysis for Measuring Crustal Deformation.” *Tectonophysics* 514-517 (2012): 1–13.

Investigation, Subsurface. 2005. “Standard Guide for Using the Surface Ground Penetrating Radar Method for Subsurface Investigation” 99 (Reapproved).

Jain, Vikrant, and R. Sinha. 2005. “Response of Active Tectonics on the Alluvial Baghmati River, Himalayan Foreland Basin, Eastern India.” *Geomorphology* 70 (3-4 SPEC. ISS.): 339–56.

Jayangondaperumal, R., J. L. Mugnier, and a. K. Dubey. 2013. “Earthquake Slip Estimation from the Scarp Geometry of Himalayan Frontal Thrust, Western Himalaya: Implications for Seismic Hazard Assessment.” *International Journal of Earth Sciences* 102 (7): 1937–55.

Jia, N., Zeng, Q. & Jiao, J., 2008. Scansar interferometry application in Dangxiong, Tibet. In European Space Agency, (Special Publication) ESA SP. pp. 2–6.

Jiang, L. et al., 2008. Monitoring crustal deformation along the xianshuihe fault in the eastern tibetan margin area with envisat scansar interferometry. In International Geoscience and Remote Sensing Symposium (IGARSS). IEEE, pp. IV – 9–IV – 12.

Jiang, L., Lin, H. & Liu, F., 2010. Application of ENVISAT ScanSAR interferometry to long-range fault creep: a case study of the Xianshuihe fault in the eastern Tibetan margin area. Annals of GIS, 16(2), pp.113–119.

Jol, H. 2009. “Ground Penetrating Radar: Theory and Applications.” In *Ground Penetrating Radar*,.

Kumahara, Yasuhiro, and R. Jayangondaperumal. 2013. “Paleoseismic Evidence of a Surface Rupture along the Northwestern Himalayan Frontal Thrust (HFT).” *Geomorphology* 180-181 (2013). Elsevier B.V.: 47–56.

Kumar Singh, a., B. Parkash, R. Mohindra, J. V. Thomas, and a. K. Singhvi. 2001. “Quaternary Alluvial Fan Sedimentation in the Dehradun Valley Piggyback Basin, NW Himalaya: Tectonic and Palaeoclimatic Implications.” *Basin Research* 13 (4): 449–71. doi:10.1046/j.0950-091x.2001.00160.x.

Kumar, S. et al., 2010. Paleoseismological evidence of surface faulting along the northeastern Himalayan front, India: Timing, size, and spatial extent of great earthquakes. *Journal of Geophysical Research: Solid Earth*, 115(12), pp.1–20.

Kumar, Senthil, and Sg Wesnousky. 2005. "The Himalayan Frontal Thrust of India Is Not Blind." *J. Geophys. …*, 1–70.

Kumar, Senthil, Steven G Wesnousky, Thomas K Rockwell, Daniel Ragona, Vikram C Thakur, and Gordon G Seitz. 2001. "Earthquake Recurrence and Rupture Dynamics of Himalayan Frontal Thrust, India." *Science (New York, N.Y.)* 294 (5550): 2328–31.

Kumar, Senthil, Steven G. Wesnousky, Thomas K. Rockwell, Richard W. Briggs, Vikram C. Thakur, and R. Jayangondaperumal. 2006. "Paleoseismic Evidence of Great Surface Rupture Earthquakes along the Indian Himalaya." *Journal of Geophysical Research: Solid Earth* 111 (3): 1–19.

Lavé, J., and J. P. Avouac. 2000. "Active Folding of Fluvial Terraces across the Siwaliks Hills, Himalayas of Central Nepal." *Journal of Geophysical Research* 105 (B3): 5735.

Le Fort, P. 1975. "Himalayas: The Collided Range. Present Knowledge of the Continental Arc." *American Journal of Science* 275: 1–44.

Liang, C, Q Zeng, J Jia, J Jiao, X Cui, and X Zhou. 2008. "ALOS PALSAR ScanSAR Interferometry and Its Application in Wenchuan Earthquake." *Fringe 2009* 2009 (March). IEEE: 1187–90.

Liang, Cunren, Qiming Zeng, Xiai Cui, and Jian Jiao. 2010. "Burst Mode to Strip-Map Mode SAR Interferometry of ALOS PALSAR." Pp. 4023–26 in *International Geoscience and Remote Sensing Symposium (IGARSS)*. IEEE.

Liu, Lanbo, and Yong Li. 2001. "Identification of Liquefaction and Deformation Features Using Ground Penetrating Radar in the New Madrid Seismic Zone , USA," 199–215.

Malik, J. N., a. K. Sahoo, and a. a. Shah. 2007. "Ground-Penetrating Radar Investigation along Pinjore Garden Fault: Implication toward Identification of Shallow Subsurface Deformation along Active Fault, NW Himalaya." *Current Science* 93 (10): 1422–27.

Malik, J. N., T. Nakata, G. Philip, N. Suresh, and N. S. Virdi. 2008. "Active Fault and Paleoseismic Investigation: Evidence of a Historic Earthquake along Chandigarh Fault in the Frontal Himalayan Zone, NW India." *Himalayan Geology* 29 (2): 109–17.

Malik, J.N. et al., 2003. Preliminary observations from a trench near Chandigarh, NW Himalaya and their bearing on active faulting. *Current Science*, 85(12), pp.1793–1798.

Malik, Javed N., Ajit K. Sahoo, Afroz a. Shah, Dattatraya P. Shinde, Navin Juyal, and Ashok K. Singhvi. 2010. "Paleoseismic Evidence from Trench Investigation along Hajipur Fault, Himalayan Frontal Thrust, NW Himalaya: Implications of the Faulting Pattern on Landscape Evolution and Seismic Hazard." *Journal of Structural Geology* 32 (3). Elsevier Ltd: 350–61.

Malik, JN, and Takashi Nakata. 2003. "Active Faults and Related Late Quaternary Deformation along the Northwestern Himalayan Frontal Zone, India." *Annals of Geophysics* 46.

Manjoro, Munyaradzi. 2015. "Structural Control of Fluvial Drainage in the Western Domain of the Cape Fold Belt, South Africa." *Journal of African Earth Sciences* 101: 350–59.

McClymont, A.F. et al., 2008. Characterization of the shallow structures of active fault zones using 3-D ground-penetrating radar data. *Journal of Geophysical Research*, 113(B10), pp.1–26.

Meschede, Martin, Ulrich Asprion, and Klaus Reicherter. 1997. “Visualization of Tectonic Structures in Shallow-Depth High-Resolution Ground-Penetrating Radar (GPR) Profiles.” *Terra Nova* 9 (4): 167–70.

Miyawaki, M. & Kimura, T., 2013. Improvement of ScanSAR interferometric processing. In 2013 IEEE International Geoscience and Remote Sensing Symposium - IGARSS. IEEE, pp. 334–337.

Miyawaki, Masanori, Shino Yamaguchi, and Tsunekazu Kimura. 2011. “Extraction of Wide-Ranging Crustal Movement Using ALOS/PALSAR ScanSAR Interferometry.” In *International Geoscience and Remote Sensing Symposium (IGARSS)*, 1187–90.

Mohanty, C., Baral, D.J. & Malik, J.N., 2004. Use of satellite data for tectonic interpretation, nw Himalaya. *Journal of the Indian Society of Remote Sensing*, 32(3), pp.241–247. Available at:

Molnar, P. 1984. “Structure and Tectonics of the Himalaya: Constraints and Implications of Geophysical Data.” *Annual Review of Earth and Planetary Sciences* 12 (1): 489–518.

Morino, M. et al., 2008. Active fault traces along Bhuj Fault and Katrol Hill fault, and Trenching survey at Wandhay, Kachchh, Gujarat, India. Journal of Earth System Science, 117(3), pp.181–188.

Mugnier, J. L., a. Gajurel, P. Huyghe, R. Jayangondaperumal, F. Jouanne, and B. Upreti. 2013. “Structural Interpretation of the Great Earthquakes of the Last Millennium in the Central Himalaya.” *Earth-Science Reviews* 127. Elsevier B.V.: 30–47.

Nakata, R S Yeats T, and A Farah M Fort. 1992. “The Himalayan Frontal Fault System.” *Annals of Geophysics* VI (Special Issue): 85–98.

Nakata, Takashi. 1972. “Geomorphic History and of Crustal Movements of the Himalayas,” *Thesis*.177.

Neal, Adrian. 2004. “Ground-Penetrating Radar and Its Use in Sedimentology: Principles, Problems and Progress.” *Earth-Science Reviews* 66 (3-4): 261–330. doi:10.1016/j.earscirev.2004.01.004.

Parkash, B., Sudhir Kumar, M. Someshwar Rao, S. C. Giri, C. Suresh Kumar, Shekhar Gupta, and Pankaj Srivastava. 2000. “Holocene Tectonic Movements and Stress Field in the Western Gangetic Plains.” *Current Science* 79 (4): 438–49.

Pernito, Mark Anthony E. 2008. “ROCK MASS SLOPE STABILITY ANALYSIS BASED ON 3D TERRESTRIAL LASER SCANNING AND GROUND PENETRATING RADAR Rock Mass Slope Stability Analysis Based on 3D Terrestrial Laser Scanning and Ground Penetrating Radar.”(P.hd. Thesis)

Philip, G., Bhakuni, S.S. & Suresh, N., 2012. Late Pleistocene and Holocene large magnitude earthquakes along Himalayan Frontal Thrust in the Central Seismic Gap in NW Himalaya, Kala Amb, India. *Tectonophysics*, 580, pp.162–177.

Philip, G., N. Suresh, and S. S. Bhakuni. 2014. “Active Tectonics in the Northwestern Outer Himalaya: Evidence of Large-Magnitude Palaeoearthquakes in Pinjaur Dun and the Frontal Himalaya.” *Current Science* 106 (2): 211–22.

Phillp, G. 1995. “Active Tectonics in the Doon Valley.” *Journal of Himalayan Geology*, 6 (2): 55–61.

Powers, Peter M., Robert J. Lillie, and Robert S. Yeats. 1998. “Structure and Shortening of the Kangra and Dehra Dun Reentrants, Sub-Himalaya, India.” *Bulletin of the Geological Society of America* 110 (8): 1010–27.

Radhakrishnan, N., 2011. Application of GPS in identifying active fault plane in Western Maharashtra Peninsular shield of India. Journal of the Geological Society of India, 77(4), pp.360–366.

Raj Rachna, et., al 2003. "Geomorphic Indicators of Active Tectonics in Karjan River Basin, Lower Narmada Valley, Western India." Geological, Journal Of, Society 62: 739–52.

Ramasamy, S. M. 2006. "Remote Sensing and Active Tectonics of South India." *International Journal of Remote Sensing* 27 (20): 4397–4431.

Ramasamy, S. M., C. J. Kumanan, R. Selvakumar, and J. Saravanavel. 2011. "Remote Sensing Revealed Drainage Anomalies and Related Tectonics of South India." *Tectonophysics* 501 (1-4). Elsevier B.V.: 41–51.

Rashed, Mohamed, and Koichi Nakagawa. 2004. "High-Resolution Shallow Seismic and Ground Penetrating Radar Investigations Revealing the Evolution of the Uemachi Fault System, Osaka, Japan." *Island Arc* 13 (1): 144–56.

Reiss, S., K. R. Reicherter, and C.-D. Reuther. 2003. "Visualization and Characterization of Active Normal Faults and Associated Sediments by High-Resolution GPR." *Geological Society, London, Special Publications* 211 (1): 247–55.

Roberts, Gerald P., Bansri Raithatha, Giancanio Sileo, Alberto Pizzi, Stefano Pucci, Joanna Faure Walker, Max Wilkinson, et al. 2010a. "Shallow Subsurface Structure of the 2009 April 6 Mw 6.3 L'Aquila Earthquake Surface Rupture at Paganica, Investigated with Ground-Penetrating Radar." *Geophysical Journal International* 183 (2): 774–90.

Rossetti, Dilce F. 2003. "Delineating Shallow Neogene Deformation Structures in Northeastern Para State Using Ground Penetrating Radar." *Anais Da Academia Brasileira de Ciencias* 75 (2): 235–48.

Salvi, S., F. R. Cinti, L. Colini, G. D'Addezio, F. Doumaz, and E. Pettinelli. 2003a. "Investigation of the Active Celano-L'Aquila Fault System, Abruzzi (central Apennines, Italy) with Combined Ground-Penetrating Radar and Palaeoseismic Trenching." *Geophysical Journal International* 155 (3): 805–18.

Srivastava, H. N., B. K. Bansal, and Mithila Verma. 2013. "Largest Earthquake in Himalaya: An Appraisal." *Journal of the Geological Society of India* 82 (1): 15–22.

Taylor, M., and a. Yin. 2009. "Active Structures of the Himalayan-Tibetan Orogen and Their Relationships to Earthquake Distribution, Contemporary Strain Field, and Cenozoic Volcanism." *Geosphere* 5 (3): 199–214.

Thakur, V. C. 2013. "Active Tectonics of Himalayan Frontal Fault System." *International Journal of Earth Sciences* 102 (7): 1791–1810.

Trifonov, Vg, and Mn Machette. 1993. "The World Map of Major Active Faults Project." *Annals of Geophysics* 36 (3-4).

Trifonov, Vladimir G, and Russian Academy. 1995. "World Map of Active Faults" *Science* 25: 3–12.

Verma, Mithila, and B. K. Bansal. 2013. "Active Fault Mapping: An Initiative towards Seismic Hazard Assessment in India." *Journal of the Geological Society of India* 82 (2): 103–6.

Wallace, Robert E. 1990. "Active Faults, Paleoseismology, and Earthquake Hazards." *U.S. Geological Survey*. U.S. Geological Survey, Menlo Park, CA 94025.

Wesnousky, Steven G, Senthil Kumar, R. Mohindra, and V. C. Thakur. 1999. "Uplift and Convergence along the Himalayan Frontal Thrust of India." *Tectonics* 18 (6): 967–76.

Yalçiner, Cahit Çağlar, Erhan Altunel, Maksim Bano, Mustapha Meghraoui, Volkan Karabacak, and H. Serdar Akyüz. 2013. "Application of GPR to Normal Faults in the Büyük Menderes Graben, Western Turkey." *Journal of Geodynamics* 65: 218–27.

Yalçiner, Cahit Çağlar, Erhan Altunel, Maksim Bano, Mustapha Meghraoui, Volkan Karabacak, and H. Serdar Akyüz. 2013. "Application of GPR to Normal Faults in the Büyük Menderes Graben, Western Turkey." *Journal of Geodynamics* 65: 218–27.

Yeats, Robert S., and Robert J. Lillie. 1991. "Contemporary Tectonics of the Himalayan Frontal Fault System. Folds, Blind Thrusts and the 1905 Kangra Earthquake." *Journal of Structural Geology* 13 (2): 227–33. doi:10.1016/0191-8141(91)90069-U.

Yetton, Mark D., and David C. Nobes. 1998. "Recent Vertical Offset and Near-surface Structure of the Alpine Fault in Westland, New Zealand, from Ground Penetrating Radar Profiling." *New Zealand Journal of Geology and Geophysics* 41 (4): 485–92.

Yin, An. 2006. "Cenozoic Tectonic Evolution of the Himalayan Orogen as Constrained by along-Strike Variation of Structural Geometry, Exhumation History, and Foreland Sedimentation." *Earth-Science Reviews* 76 (1-2): 1–131.

Yoshioka, Toshikazu. 2009. "Evaluation of Earthquake Occurrence from Active Faults." *Synthesiology English Edition*. doi:10.5571/syntheng.2.177.

Internet Sources:

1. **http://diss.rm.ingv.it/diss/UserManual-ActiveFault.html**
2. **http://www.nsr.go.jp/archive/nsc/NSCenglish/topics/seismic_safety/Column5.pdf**
3. **http://www.gns.cri.nz/Home/Learning/Science-Topics/Earthquakes/Earthquakes-and-Faults/When-is-a-Fault-Active**

APPENDIX- 1

The Field photographs collected at GPR Sites.

In above figure- 'A' Boulder beds and B clayey-sand shows the omission of bed 'B' towards right side near Abhipur Village (30.89° N, 76.67°E), Punjab.

Arrow showing uplifted clay bed and black line showing probable fault near Abhipur Village (30.89° N, 76.67°E), Punjab.

Above figure shows discontinuity in bed in Abhipur.

Line showing a probable fault between two different beds (Boulder and Clay) near Govindpur along Thakar ka Nala (30.601484°N, 77.071124°E) in Haryana. Right top of the figure showing a sag pond giving the evidence of faulting.

Some field evidences of deformation near Kala-Amb.

Above figure shows (A) Strike slip movement of bed (B) Slickensides (C) Triangular facets near fault plane and (D) Intrusion of clay layer in the fault plane.